

High levels of primary biogenic organic aerosols are driven by only a few plant-associated microbial taxa

Abdoulaye Samaké^{1*}, Aurélie Bonin², Jean-Luc Jaffrezo¹, Pierre Taberlet², Samuël Weber¹, Gaëlle Uzu¹, Véronique Jacob¹, Sébastien Conil³, Jean M. F. Martins^{1*}

¹University Grenoble Alpes, CNRS, IRD, INP-G, IGE (UMR 5001), 38000 Grenoble, France

²University Grenoble Alpes, CNRS, LECA (UMR 5553), BP 53, 38041 Grenoble, France

³ANDRA DRD/OPE Observatoire Pérenne de l'Environnement, 55290 Bure, France

* *Corresponding to:* Abdoulaye Samaké (abdoulaye.samake2@univ-grenoble-alpes.fr) and Jean Martins (jean.martins@univ-grenoble-alpes.fr)

1 **Abstract.** Primary biogenic organic aerosols (PBOA) represent a major fraction of coarse organic matter (OM) in
2 air. Despite their implication in many atmospheric processes and human health problems, we surprisingly know
3 little about PBOA characteristics (i.e., composition, dominant sources, and contribution to airborne-particles). In
4 addition, specific primary sugar compounds (SCs) are generally used as markers of PBOA associated with bacteria
5 and fungi but our knowledge of microbial communities associated with atmospheric particulate matter (PM)
6 remains incomplete. This work aimed at providing a comprehensive understanding of the microbial fingerprints
7 associated with SCs in PM₁₀ (particles smaller than 10µm) and their main sources in the surrounding environment
8 (soils and vegetation). An intensive study was conducted on PM₁₀ collected at rural background site located in an
9 agricultural area in France. We combined high-throughput sequencing of bacteria and fungi with detailed
10 physicochemical characterization of PM₁₀, soils and plant samples, and monitored meteorology and agricultural
11 activities throughout the sampling period. Results shows that in summer SCs in PM₁₀ are a major contributor of
12 OM in air, representing 0.8 to 13.5% of OM mass. SCs concentrations are clearly determined by the abundance of
13 only a few specific airborne fungi and bacteria taxa. The temporal fluctuations in the abundance of only 4
14 predominant fungal genera, namely *Cladosporium*, *Alternaria*, *Sporobolomyces* and *Dioszegia* reflect the temporal
15 dynamics in SC concentrations. Among bacteria taxa, the abundance of only *Massilia*, *Pseudomonas*,
16 *Frigoribacterium* and *Sphingomonas* are positively correlated with SC species. These microbial are significantly
17 enhanced in leaf over soil samples. Interestingly, the overall community structure of bacteria and fungi are similar
18 within PM₁₀ and leaf samples and significantly distinct between PM₁₀ and soil samples, indicating that surrounding
19 vegetation are the major source of SC-associated microbial taxa in PM₁₀ on rural area of France.

20 1. Introduction

21 Airborne particulate matter (PM) is the subject of high scientific and political interests mainly because of its
22 important effects on climate and public health (Boucher et al., 2013; Fröhlich-Nowoisky et al., 2016; Fuzzi et al.,
23 2006). Numerous epidemiological studies have significantly related both acute and chronic exposures to ambient
24 PM with respiratory impairments, heart diseases, asthma, lung cancer, as well as increased risk of mortality (Kelly
25 and Fussell, 2015; Pope and Dockery, 2006). PM can also affect directly or indirectly the climate by absorbing
26 and/or diffusing both the incoming and outgoing solar radiation (Boucher et al., 2013; Fröhlich-Nowoisky et al.,
27 2016). These effects are modulated by highly variable physical characteristics (e.g., size, specific surface,
28 concentrations, etc.) and complex chemical composition of PM (Fröhlich-Nowoisky et al., 2016; Fuzzi et al.,
29 2015). PM consists of a complex mixture of inorganic, trace elements and carbonaceous matter (organic carbon
30 and elemental carbon) with organic matter (OM) being generally the major but poorly characterized constituent of
31 PM (Boucher et al., 2013; Bozzetti et al., 2016). A quantitative understanding of OM sources is critically important
32 to develop efficient guidelines for both air quality control and abatement strategies. So far, considerable efforts
33 have been undertaken to investigate OM associated with anthropogenic and secondary sources, but much less is
34 known about emissions from primary biogenic sources (Bozzetti et al., 2016; China et al., 2018; Yan et al., 2019).

35 Primary biogenic organic aerosols (PBOAs) are a subset of organic PM that are directly emitted by processes
36 involving the biosphere (Boucher et al., 2013; Elbert et al., 2007). PBOAs refer typically to biologically derived
37 materials, notably including living organisms (bacteria, fungal spores, Protozoa, viruses) and non-living biomass
38 (e.g., microbial fragments) and other types of biological materials like pollen or plant debris (Amato et al., 2017;
39 Elbert et al., 2007; Fröhlich-Nowoisky et al., 2016). PBOAs are gaining increasing attention notably because of
40 their ability to affect human health by causing infectious, toxic, and hypersensitivity diseases (Fröhlich-Nowoisky
41 et al., 2016; Huffman et al., 2019). For instance, PBOA components, especially fungal spores and bacterial cells,
42 have recently been shown to cause significant oxidative potential (Samaké et al., 2017). However, to date, the
43 precise role of PBOA components and interplay regarding mechanisms of diseases are remarkably misunderstood
44 (Coz et al., 2010; Hill et al., 2017). Specific PBOA components can also participate in many relevant atmospheric
45 processes like cloud condensation and ice nucleation, thereby directly or indirectly affecting the Earth's
46 hydrological cycle and radiative balance (Boucher et al., 2013; Fröhlich-Nowoisky et al., 2016; Hill et al., 2017).
47 These diverse impacts are effective at a regional scale due to the transport of PBOAs (Dommergue et al., 2019;
48 Yu et al., 2016). Moreover, PBOAs are a major component of OM found in particles less than 10 µm in
49 aerodynamic diameter (PM₁₀) (Bozzetti et al., 2016; Coz et al., 2010; Samaké et al., 2019b). For instance, Bozzetti
50 et al. (2016) have shown that PBOAs equal the contribution of secondary organic aerosols (SOAs) to OM in PM₁₀
51 collected at a rural background site in Switzerland during both the summer and winter periods. However, current
52 estimates of global terrestrial PBOA emissions are very uncertain and range between 50 and 1000 Tg y⁻¹ (Boucher

53 et al., 2013; Coz et al., 2010; Elbert et al., 2007), underlining the critical gap in the understanding of this significant
54 OM fraction.

55 The recent application of fluorescent technics such as ultraviolet aerodynamic particle sizer, wideband integrated
56 bioaerosol sensor (Bozzetti et al., 2016; Gosselin et al., 2016; Huffman and Santarpia, 2017; Huffman et al., 2019),
57 or scanning electron microscopy (Coz et al., 2010) have provided very insightful information on the abundance of
58 size segregated ambient PBOAs. Atmospheric sources of PBOAs are numerous and include agricultural activities,
59 leaf abrasion, and soil resuspension. (Coz et al., 2010; Medeiros et al., 2006; Pietrogrande et al., 2014). To date,
60 the detailed constituents of PBOAs, their predominant sources and atmospheric emission processes as well as their
61 contributions to total airborne particles remain poorly documented and quantified (Bozzetti et al., 2016; Coz et al.,
62 2010; Elbert et al., 2007). Such information would be important for investigating the properties and atmospheric
63 impacts of PBOAs as well as for a future optimization of source-resolved chemical transport models (CTM), which
64 are still generally unable to accurately simulate important OM fractions (Ciarelli et al., 2016; Heald et al., 2011;
65 Kang et al., 2018).

66 Primary sugar compounds (SC, defined as sugar alcohols and saccharides) are ubiquitous water-soluble
67 compounds found in atmospheric PM (Gosselin et al., 2016; Medeiros et al., 2006; Pietrogrande et al., 2014; Jia
68 et al., 2010b). SC species are emitted from biologically derived sources (Medeiros et al., 2006, Verma et al., 2018)
69 and have sometimes been detected in aerosols taken from air masses influenced by smoke from biomass burning
70 (Fu et al., 2012; Yang et al., 2012). However, recent studies conducted at several sites across France revealed a
71 weak correlation between daily concentrations of SC and levoglucosan in PM_{2.5} and PM₁₀ collected throughout
72 the year (Golly et al., 2018; Samaké et al., 2019a). This suggests that open burning of biomass is not a significant
73 source of SC in the environments studied here. In this context, specific SC species are still extensively viewed as
74 powerful markers for tracking sources and estimating PBOA contributions to OM mass (Bauer et al., 2008;
75 Gosselin et al., 2016; Jia et al., 2010b; Medeiros et al., 2006). For example, glucose is the most common
76 monosaccharide in vascular plants and it has been predominantly used as indicator of plant material (such as pollen
77 or plant debris) from several areas around the world (Jia et al., 2010b; Medeiros et al., 2006; Pietrogrande et al.,
78 2014; Verma et al., 2018). Trehalose (aka mycose) is a common metabolite of various microorganisms, serving as
79 an osmoprotectant accumulating in cells cytosol during harsh conditions (e.g., dehydration and heat) (Bougouffa
80 et al., 2014). It has been proposed as a generic indicator of soil-borne microbiota (Jia et al., 2010b; Medeiros et
81 al., 2006; Pietrogrande et al., 2014; Verma et al., 2018). Similarly, mannitol and arabitol are two very common
82 sugar alcohols (also called polyols) serving as storage and transport solutes in fungi (Gosselin et al., 2016;
83 Medeiros et al., 2006; Verma et al., 2018). Their atmospheric concentrations levels have frequently been used to
84 investigate fungal spores contributions to PBOAs mass in different environments (urban, rural, costal, and polar)
85 around the world (Barbaro et al., 2015; Gosselin et al., 2016; Jia et al., 2010b; Verma et al., 2018; Weber et al.,
86 2018).

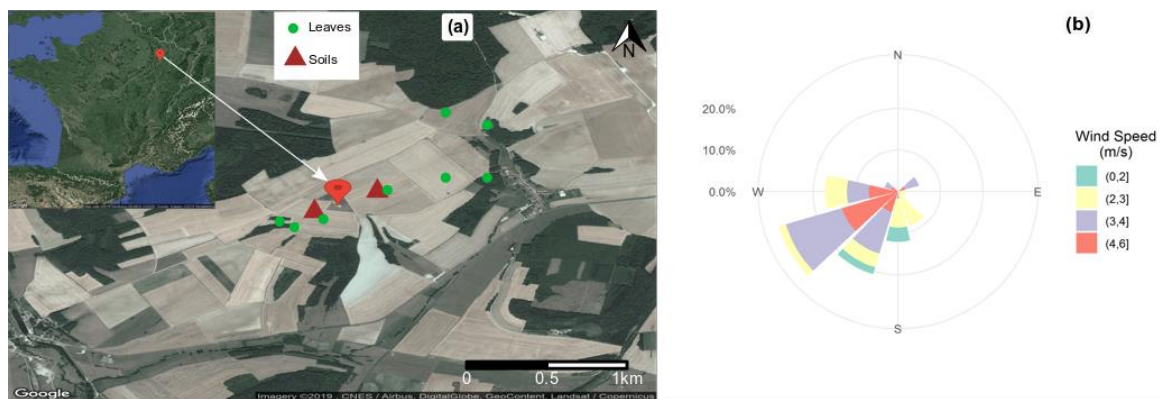
87 Despite the relatively vast literature using the atmospheric concentration levels of SC as potential suitable markers
88 of PBOAs associated with bacteria and fungi, our understanding of associated airborne microbial communities
89 (i.e., diversity and community composition) remains poor. This is due in particular to the lack of high-resolution
90 (i.e., daily) data sets characterizing how well the variability of these microbial communities may be related to that
91 of primary sugar species. Such information is of paramount importance to better understand the dominant
92 atmospheric sources of SC (and then PBOAs) as well as their relevant effective environmental drivers, which are
93 still poorly documented (Bozzetti et al., 2016).

94 Our recent works discussed the size distribution features as well as the spatial and temporal variability in
95 atmospheric particulate SC concentrations in France (Golly et al., 2018; Samaké et al., 2019a, 2019b). As a
96 continuation, in this study, we present the first daily temporal concurrent characterization of ambient SC species
97 concentrations and both bacterial and fungal community compositions for PM₁₀ collected at a rural background
98 site located in an intensive agricultural area. The aim of this study was to use a DNA metabarcoding approach
99 (Taberlet et al., 2018) to investigate PM₁₀-associated microbial communities, which can help answering the
100 following research questions: (i) What are the microbial community structures associated with PM₁₀? (ii) Is the
101 temporal dynamics of SC concentrations related to changes of the airborne microbial community compositions?
102 (iii) What are the predominant sources of SC-associated microbial communities at a continental rural field site?
103 Since soil and vegetation are currently believed to be the dominant sources of airborne microorganisms in most
104 continental areas (Bowers et al., 2011; Jia et al., 2010a; Rathnayake et al., 2016), our study focused on these two
105 potential sources.

106 2. Material and methods

107 2.1. Site description

108 The Observatoire Pérenne de l'Environnement (OPE) is a continental rural background observatory located at
109 about 230 km east of Paris at an altitude of 392 m (Fig. 1). This French Critical Zone Observatory (CZO) is part
110 of a long term multi-disciplinary project monitoring the state of environmental variables including among other
111 fluxes, abiotic and biotic variables, and their functions and dynamics (<http://ope.andra.fr/index.php?lang=en>, last
112 access: December 10, 2019). It is largely impacted by agricultural activities. It is also characterized by a low
113 population density (less than 22 per km² within an area of 900 km²), with no industrial activities nor surrounding
114 major transport road. The air monitoring site itself lies in a “*reference sector*” of 240 km², in the middle of a field
115 crop area (tens of kilometers in all directions). This reference sector is composed of vast farmlands interspersed
116 with wooded areas. The area is further defined by a homogeneous soil type, with a predominantly superficial clay-
117 limestone composition. The daily agricultural practices and meteorological data (including wind speed and
118 direction, temperature, rainfall level and relative humidity) within the reference sector are recorded and made
119 available by ANDRA (Agence nationale pour la gestion des déchets radioactifs). The agricultural fields of the area
120 are generally submitted to a 3-year crop-rotation system. The major crops during the campaign period were pea
121 and oilseed rape.
122



123
124 **Figure 1 : Overview of the sampling area at the OPE site (France). (A) Location of sampling units and (B) wind**
125 **conditions (speed and direction) during the field sampling campaign period.**

126 2.2. Samples collection

127 An intensive field campaign was conducted at this site for the sake of the present study. The aerosol sampling
128 campaign period lasted from June 12th to August 21st, 2017, covering the summer period in France. During this
129 period, ambient PM₁₀ were collected daily (starting at 9 am UTC to 9 am UTC the next day) onto prebaked quartz
130 fiber filters (Tissuquartz PALL QAT-UP 2500, Ø = 150 mm) using high volume samplers (Aerosol Sampler DHA-
131 80, Digitel; 24 h at 30 m³ h⁻¹). After collection, all filter samples were wrapped in aluminum foils, sealed in zipper
132 plastic bags, and stored at < 4 °C until further analysis. More details on the preparation, storage, and handling of
133 these filter samples can be found in Samaké et al. (2019b). A total of 69 samples and six field blanks were collected.

134 Surface soil samples (0-5 cm depth, 15x15 cm area) were simultaneously collected from two fields, within pea
135 and oilseed rape-growing areas, respectively. The fields are located in the immediate vicinity of the PM₁₀ sampler
136 and under the prevailing wind directions (Fig. 1). To represent as closely as possible the local soil microbial
137 communities, we randomly collected five subsamples (about 100g per sampling unit) within each parcel and
138 pooled them. Topsoil sampling took place on a weekly basis along the campaign period. After collection and
139 homogenization, 15g of each subsample were stored in airtight containers (sterile bottles, Schott, GL45, 100ml)
140 containing the same weight of sterile silica gel (around 15g). Such soil desiccation method is a straightforward
141 approach to prevent any microbial growth and change in community over time at room temperature (Taberlet et
142 al., 2018). A total of eight topsoil samples were collected for each parcel.

143 Finally, leaf samples were collected from the major types of vegetables within the reference sector. These include
144 leaf of oilseed rape, pea, oak, maples, beech, and herbs (Fig. 1). A total of eight leaf samples were analyzed. These
145 samples were also stored in airtight containers (sterile bottles, Schott, GL45, 100ml) containing 15g of silica gel.

146 It should be noted that leaf samples were collected only once, four weeks after the end of PM and soil sampling,
147 while the major crops were still on site.

148 **2.3. Chemical analyses**

149 Daily PM₁₀ samples were analyzed for various chemical species using subsampled fractions of the collection filters
150 and a large array of analytical methods. Detailed information on all the chemical analysis procedures have been
151 reported previously (Golly et al., 2018; Samaké et al., 2019b; Waked et al., 2014). Briefly, SCs (i.e. polyols and
152 saccharides) and water-soluble ions (including Ca²⁺) have been systematically analyzed in all samples, using
153 respectively high-performance liquid chromatography with pulsed amperometric detection (HPLC-PAD) and
154 ionic chromatography (IC, Thermo Fisher ICS 3000, USA). Free-cellulose concentrations were determined using
155 an optimized enzymatic hydrolysis (Samaké et al., 2019a) and the subsequent analysis method of the resultant
156 glucose units with an HPLC-PAD (Golly et al., 2018; Samaké et al., 2019b; Waked et al., 2014). Organic and
157 elemental carbon (OC, EC) have been analyzed using a Sunset thermo-optic instrument and the EUSAAR2
158 protocol (Cavalli et al., 2010). This analytical method requires high temperature, thereby constraining the choice
159 of quartz as sampling filter material. OM content in PM₁₀ samples were then estimated using an OM-to-OC
160 conversion factor of 1.8: $OM = 1.8 \times OC$ (Samaké et al., 2019b, 2019a). This value of 1.8 for the OM/OC ratio
161 was chosen on the basis of previous studies carried out in France (Samaké et al., 2019b, and reference therein)

162 **2.4. Biological analyses: DNA extraction in PM₁₀ samples**

163 Aerosol samples typically contain very low DNA concentrations, and the DNA-binding properties of quartz fibers
164 of aerosol collection filters make challenging its extraction with traditional protocols (Dommergue et al., 2019;
165 Jiang et al., 2015; Luhung et al., 2015). In the present study, we were also constrained by the limited available
166 daily collection filter surface for simultaneous chemical and microbiological analyses of the same filters. To
167 circumvent issues of low efficiency during genomic DNA extraction, several technical improvements have been
168 made to optimize the extraction of high-quality DNA from PM₁₀ samples (Dommergue et al., 2019; Jiang et al.,
169 2015; Luhung et al., 2015). These include thermal water bath sonication helping lysis of thick cell walls (e.g.,
170 fungal spores and gram-positive bacteria), which might not be effectively lysed by means of sole bead beating
171 (Luhung et al., 2015). Some consecutive (2 days at maximum) quartz filter samples with low OM concentrations
172 were also pooled when necessary. Detailed information regarding the resultant composite samples (labeled as A1
173 to A36) are presented in Table S1. Figure S1 presents the average concentration levels of SC species in each
174 sample. The results clearly show that air samples can be categorized from low (background, from A1 to A4 and
175 A21 to A36) to high (peak, from A5 to A20) PM₁₀ SC concentration levels.

176 In terms of DNA extraction, ¼ (about 38.5 cm²) of each filter sample were used. First, filter aliquots were
177 aseptically inserted into individual 50 mL Falcon tubes filed with sterilized saturated phosphate buffer (Na₂HPO₄,
178 NaH₂PO₄, 0.12 M; pH ≈ 8). PM₁₀ were desorbed from the filter samples by gentle shaking for 10 min at 250 rpm.
179 This pretreatment allows the separation of the collected particles from quartz filters thanks to the high competing
180 interaction between saturated phosphate buffer and charged biological materials (Jiang et al., 2015; Taberlet et al.,
181 2018). After gentle vortex mixing, the subsequent resuspension was filtered with a polyethersulphone membrane
182 disc filter (PES, Supor® 47mm 200, 0.2 µm, PALL, USA). We repeated this desorbing step three times to enhance
183 the recovery of biological material from quartz filters. Each collection PES membrane was then shred into small
184 pieces and used for DNA extractions using the DNeasy PowerWater kit (Qiagen, Germantown, MD, USA). The
185 standard protocol of the supplier was followed, with only minor modifications: 30 min of thermal water bath
186 sonication at 65°C (EMAG, Emmi-60 HC, Germany; 50% of efficiency), and 5 min of bead beating before and
187 after sonication were added. Finally, DNA was eluted in 50 µl of EB buffer. Such an optimized protocol has been
188 recently shown to produce a 10-fold increase in DNA extraction efficiency (Dommergue et al., 2019; Luhung et
189 al., 2015), thereby allowing high-throughput sequencing of air samples. Note that all the steps mentioned above
190 were performed under laminar flow hoods, and that materials (filter funnels, forceps, and scissors) were sterilized
191 prior to use.

192 **2.4.1. Biological analyses: DNA extraction from soil and leaf samples**

193 The soil samples pretreatment and extracellular DNA extraction were achieved following an optimized protocol
194 proposed elsewhere (Taberlet et al., 2018). Briefly, this protocol involves mixing thoroughly and extracting 15g
195 of soil in 15 ml of sterile saturated phosphate buffer for 15 min. About 2 mL of the resulting extracts were

196 centrifuged for 10 min at 10,000g, and 500 µL of the resulting supernatant were used for DNA extraction using
197 the NucleoSpin Soil Kit (Macherey-Nagel, Düren, Germany) following the manufacturer's original protocol after
198 skipping the cells lysis step. Finally, DNA was eluted with 100 µL of SE buffer.

199 To extract DNA from either endophytic or epiphytic microorganisms, aliquots of leaf samples (about 25–30mg)
200 were extracted with the DNeasy Plant Mini Kit (QIAGEN, Germany) according to the supplier's instructions, with
201 the following minor modifications: after the resuspension of powdered samples in 400 µL of AP1 buffer, the
202 samples were incubated for 45 min at 65°C with RNase A. Finally, DNA was eluted with 100 µL of AE buffer.

203 **2.4.2. Biological analyses: PCR amplification and sequencing**

204 Bacterial and fungal community compositions were surveyed using respectively the Bact02 (Forward 5'—
205 KGCCAGCMGCCGCGGTAA—3' and Reverse 3'—GGACTACCMGGGTATCTAA—5') and Fung02
206 (Forward 5'—GGAAGTAAAAGTCGTAACAAGG—3' and Reverse 3'—
207 CAAGAGATCCGTTGYTGAAAGTK—5') published primer pairs [see (Taberlet et al., 2018) for details on
208 these primers]. The primer pair Bact02 targets the V4 region of the bacterial 16S rDNA region while the Fung02
209 primer pair targets the nuclear ribosomal internal transcribed spacer region 1 (ITS1). Four independent PCR
210 replicates were carried out for each DNA extract. Eight-nucleotide tags were added to both primer ends to uniquely
211 identify each sample, ensuring that each PCR replicate is labeled by a unique combination of forward and reverse
212 tags. The tag sequence were created with the *oligotag* command within the open-source OBITools software suite
213 (Boyer et al., 2016), so that all pairwise tag combinations were differentiated by at least five different base pairs
214 (Taberlet et al., 2018).

215 DNA amplification was performed in a 20-µL total volume containing 10 µL of AmpliTaq Gold 360 Master Mix
216 (Applied Biosystems, Foster City, CA, USA), 0.16 µL of 20 mg ml⁻¹ bovine serum albumin (BSA; Roche
217 Diagnostics, Basel, Switzerland), 0.2 µM of each primer, and 2 µL of diluted DNA extract. DNA extracts from
218 soil and filters were diluted eight times while DNA extracts from leaves were diluted four times. Amplifications
219 were performed using the following thermocycling program: an initial activation of DNA polymerase for 10 min
220 at 95°C; x cycles of 30 s denaturation at 95°C, 30 s annealing at 53°C and 56°C for bacteria and fungi, respectively,
221 90 s elongation at 72°C; and a final extension at 72°C for 7 min. The number of cycles x was determined by qPCR
222 and set at 40 for all markers and DNA extract types, except for the Bact02 amplification of soil and leaf samples
223 (30 cycles), and the Fung02 amplification of filter samples (42 cycles). After amplification, about 10% of
224 amplification products were randomly selected and verified using a QIAxel Advance device (QIAGEN, Hilden,
225 Germany) equipped with a high-resolution cartridge for separation.

226 After amplification, PCR products from the same marker were pooled in equal volumes and cleaned with the
227 MinElute PCR purification kit (Qiagen, Hilden, Germany) following the manufacturer's instructions. The two
228 pools were sent to Fasteris SA (Geneva, Switzerland; <https://www.fasteris.com/dna/>; last access December 10,
229 2019) for library preparation and MiSeq Illumina 2×250 bp paired-end sequencing. The two sequencing libraries
230 (one per marker) were prepared according to the PCR-free MetaFast protocol (www.fasteris.com/metafast, last
231 access December 10, 2019), which aims at limiting the formation of chimeras.

232 To monitor any potential false positives inherent to tag jumps and contaminations (Schnell et al., 2015), sequencing
233 experiment included both extraction and PCR negatives, as well as unused tag combinations.

234 **2.4.3. Bio-informatic analyses of raw reads**

235 The Illumina raw sequence reads were processed separately for each library using the OBITools software suite
236 (Boyer et al., 2016), specifically dedicated to metabarcoding data processing. First, the raw paired-ends were
237 assembled using the *illuminapairedend* program, and the sequences with a low alignment score (fastq average
238 quality score < 40) were discarded. The aligned sequences were then assigned to the corresponding PCR replicates
239 with the program *ngsfilter*, by allowing zero and two mismatches on tags and primers, respectively. Strictly
240 identical sequences were dereplicated using the program *obuniq*, and a basic filtration step was performed with
241 the *obigrep* program to select sequences within the expected range length (i.e., longer than 65 or 39 bp for fungi
242 and bacteria, respectively, excluding tags and primers), without ambiguous nucleotides, and observed at least 10
243 times in at least one PCR replicate.

244 The remaining unique sequences were grouped and assigned to Molecular Taxonomic Units (MOTUs) with a 97%
245 sequence identity using the *Sumatra* and *Sumaclus* programs (Mercier et al., 2013). The *Sumatra* algorithm
246 computes pairwise similarities among sequences based on the length of the Longest Common Subsequence and
247 the *Sumaclus* program uses these similarities to cluster the sequences (Mercier et al., 2013). Abundance of
248 sequences belonging to the same cluster were summed up and the cluster center was defined as the MOTU
249 representative of the cluster (Mercier et al., 2013).

250 The taxonomic classification of each MOTU was performed using the *ecotag* program (Boyer et al., 2016), which
251 uses full-length metabarcodes as references. The *ecoPCR* program (Ficetola et al., 2010) was used to build the
252 metabarcode reference database for each marker. Briefly, *ecoPCR* performs an *in silico* amplification within the
253 EMBL public database (release 133) using the Fung02 and Bact02 primer pairs and allowing a maximum of three
254 mismatches per primer. The resultant reference database was further refined by keeping only sequence records
255 assigned at the species, genus and family levels.

256 After taxonomic assignment datasets were acquired, further processing with the open source R software (R studio
257 interface, version 3.4.1) was performed to filter out chimeras, potential contaminants, chimeras and failed PCR
258 replicates. More specifically, MOTUs that were highly dissimilar to any reference sequence (sequence identity <
259 0.95) were considered as chimeras and discarded. Secondly, MOTUs whose abundance was higher in extraction
260 or PCR negatives were also excluded. Finally, PCR replicates inconstantly distant from the barycenter of the four
261 PCR replicates corresponding to the same sample were considered as dysfunctional and discarded. The remaining
262 PCR replicates were summed up per sample.

263 2.5. Data analysis

264 Unless specified otherwise, all exploratory statistical analyses were achieved with R. Rarefaction and extrapolation
265 curves were obtained with the *iNext* 2.0-12 package (Hsieh et al., 2016), to investigate the gain in species richness
266 as we increased the sequencing depth for each sample. Alpha diversity estimators including Shannon and Chao1
267 were calculated with the *phyloseq* 1.22-3 package (McMurdie and Holmes, 2013), on data rarefied to the same
268 sequencing depth per sample type (see Table S2 for details on the rarefaction depths). Non-metric
269 multidimensional scaling (NMDS) ordination analysis was performed to decipher the temporal patterns in airborne
270 microbial community structures (phylum or class taxonomic group) in air samples. These analyses were achieved
271 with the *metaMDS* function within the *vegan* package (Oksanen et al., 2019) with the number random starts set to
272 500. The NMDS ordinations were obtained using pairwise dissimilarity matrices based on Bray Curtis index. The
273 *envfit* function implemented in *vegan* was used to assess the airborne microbial communities that could explain
274 the temporal dynamics of ambient SC species concentrations. Pairwise analysis of similarity (ANOSIM) was
275 performed to assess similarity between groups of PM₁₀ aerosols sample. This was achieved using the *anosim*
276 function of *vegan* (Oksanen et al., 2019), with the number of permutations sets to 999. Spearman's rank correlation
277 analysis was used to investigate further the relationship between airborne microbial communities and SC species.

278 To gain further insight into the dominant source of SC-associated microbial communities, NMDS analysis based
279 on Horn distance was performed to compare the microbial community composition similarities between PM₁₀
280 aerosols, soils, and leaf samples.

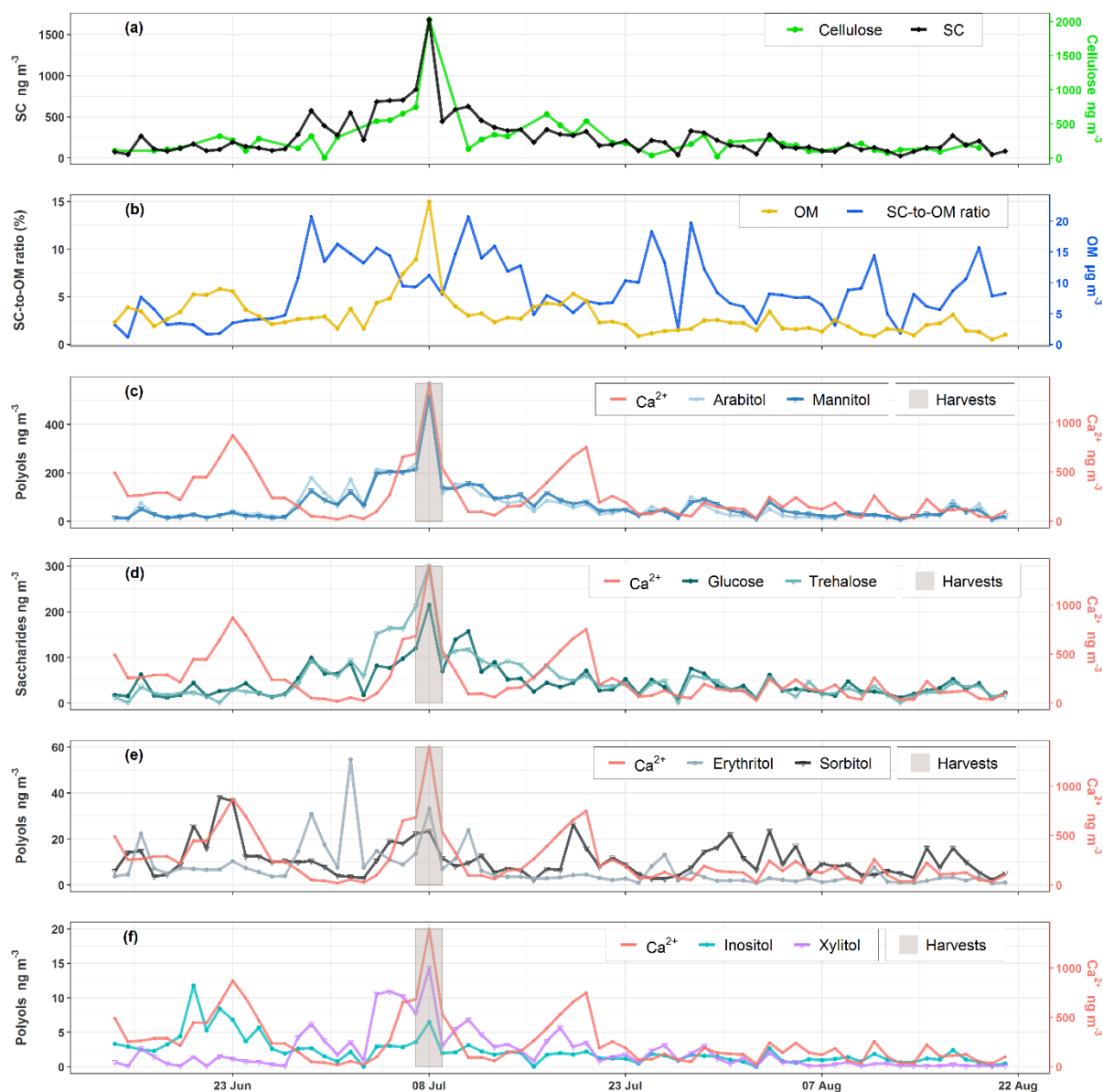
281 3. Results

282 3.1. Primary sugar compounds (SC), and relative contributions to OM mass

283 Temporal dynamics of daily PM₁₀ carbonaceous components (e.g., primary sugar compounds, cellulose and OM)
284 are presented in Fig. 2. Nine SCs including seven polyols and two saccharide compounds have been quantified in
285 all ambient PM₁₀ collected at the study site. Ambient SC concentration levels peaked on August 8th, 2017, in
286 excellent agreement with the daily harvest activities around the study site (Fig. 2A). The average concentrations
287 (average ± SD) of total SCs during the campaign are 259.8 ± 253.8 ng m⁻³, with a range of 26.6 to 1 679.5 ng m⁻³,
288 contributing on average to 5.7 ± 3.2% of total OM mass in PM₁₀, with a range of 0.8–13.5% (Fig. 2B). The total
289 measured polyols present average concentrations of 26.3 ± 54.4 ng m⁻³. Among all the measured polyols, arabitol
290 (67.4 ± 83.1 ng m⁻³) and mannitol (68.1 ± 75.3 ng m⁻³) are the predominant species, followed by lesser amounts
291 of sorbitol (10.9 ± 7.6 ng m⁻³), erythritol (7.0 ± 8.8 ng m⁻³), inositol (2.3 ± 2.0 ng m⁻³), and xylitol (2.3 ± 3.0 ng m⁻³).

292 ³). Glycerol was also observed in our samples, but with concentrations frequently below the quantification limit.
 293 The average concentrations of saccharide compounds are $51.2 \pm 45.0 \text{ ng m}^{-3}$. Threolose ($55.8 \pm 51.9 \text{ ng m}^{-3}$) is the
 294 most abundant saccharide species, followed by glucose ($46.9 \pm 37.1 \text{ ng m}^{-3}$). The average concentrations of
 295 calcium are $251.1 \pm 248.4 \text{ ng m}^{-3}$.

296 A Spearman's rank correlation analysis based on the daily dynamics was used to examine the relationships between
 297 SC species. As shown in Table 1, sorbitol and inositol are well linearly correlated ($R = 0.57, p < 0.001$). Herein,
 298 sorbitol ($R = 0.59, p < 0.001$) and inositol ($R = 0.64, p < 0.001$) are significantly correlated to Ca^{2+} . It can also be
 299 noted that all other SC species are highly correlated with each other ($p < 0.001$) and that they are weakly correlated
 300 to the temporal dynamics of sorbitol and inositol (Table 1).



301 **Figure 2: Ambient concentrations of carbonaceous components in PM₁₀. (A; C to F) Daily variations of SCs and calcium**
 302 **concentrations along with daily agricultural activities around the site. (B) Contribution of SCs to organic matter mass.**
 303 **Results for nine-week daily measurements indicate that SCs together represent a large fraction of OM, contributing**
 304 **between 0.8 to 13.5% to OM mass in summer. Glycerol is not presented because its concentration was generally below**
 305 **the quantification limit.**

307
 308
 309

310 **Table 1 : Relationships between SCs and calcium in PM₁₀ from the study site. Spearman's rank correlation analyses**
 311 **are based on the daily dynamics of chemicals species (n= 69).**

	Arabitol	Mannitol	Glucose	Trehalose	Erythritol	Xylitol	Sorbitol	Inositol	Ca ²⁺
Arabitol	1.00								
Mannitol	0.94***	1.00							
Glucose	0.90***	0.90***	1.00						
Trehalose	0.93***	0.96***	0.87***	1.00					
Erythritol	0.69***	0.51***	0.57***	0.56***	1.00				
Xylitol	0.84***	0.84***	0.80***	0.79***	0.65***	1.00			
Sorbitol	0.22	0.26*	0.35**	0.15	0.21	0.24*	1.00		
Inositol	0.39**	0.24	0.34**	0.25*	0.71***	0.39**	0.57***	1.00	
Ca ²⁺	0.12	0.11	0.11	0.09	0.30*	0.27*	0.59***	0.64***	1.00
Note	* p < 0.1	** p < 0.01	*** p < 0.001						

312

313 3.2. Microbial characterization of samples, richness and diversity

314 The structures of bacterial and fungal communities were generated for the 62 collected samples, consisting of 36
 315 aerosol, 18 surface soil, and 8 leaf samples. After paired-end assembly of sequence reads, sample assignment,
 316 filtering based on sequence length and quality and discarding of rare sequences, we are left with 2,575,857 and
 317 1,647,000 reads respectively for fungi and bacteria, corresponding respectively to 4,762 and 5,852 unique
 318 sequences, respectively. After the clustering of high-quality sequences, potential contaminants and chimeras, the
 319 final data sets (all samples pooled) consist respectively of 597 and 944 MOTUs for fungi and bacteria, with
 320 1,959,549 and 901,539 reads. The average numbers of reads (average \pm SE) per sample are $31,607 \pm 2,072$ and
 321 $14,563 \pm 1,221$, respectively. The rarefaction curves of MOTU diversity showed common logarithmic shapes
 322 approaching a plateau in all cases (Fig. S2). This indicates an overall sufficient sequencing depth to capture the
 323 diversity of sequences occurring in the different types of samples. To compare the microbial community diversity
 324 and species richness, data normalization was performed out by selecting randomly from each sample 4,287 fungal
 325 sequences and 2,865 bacterial sequence reads. The Chao1-values of fungi are higher for aerosol samples than for
 326 soil and leaf samples ($p < 0.05$), indicating higher richness in airborne PM₁₀ (Fig. S3A). In contrast, PM₁₀ and soil
 327 samples showed higher values of Shannon index ($p < 0.05$), indicating a higher fungal diversity in these
 328 ecosystems. The soil harbors higher bacterial richness and diversity than PM₁₀ ($p < 0.05$), which in turns harbors
 329 greater richness and diversity compared to leaf samples ($p < 0.05$) (Fig. S3B).

330 3.3. Taxonomic composition of airborne PM₁₀

331 3.3.1. Fungal communities

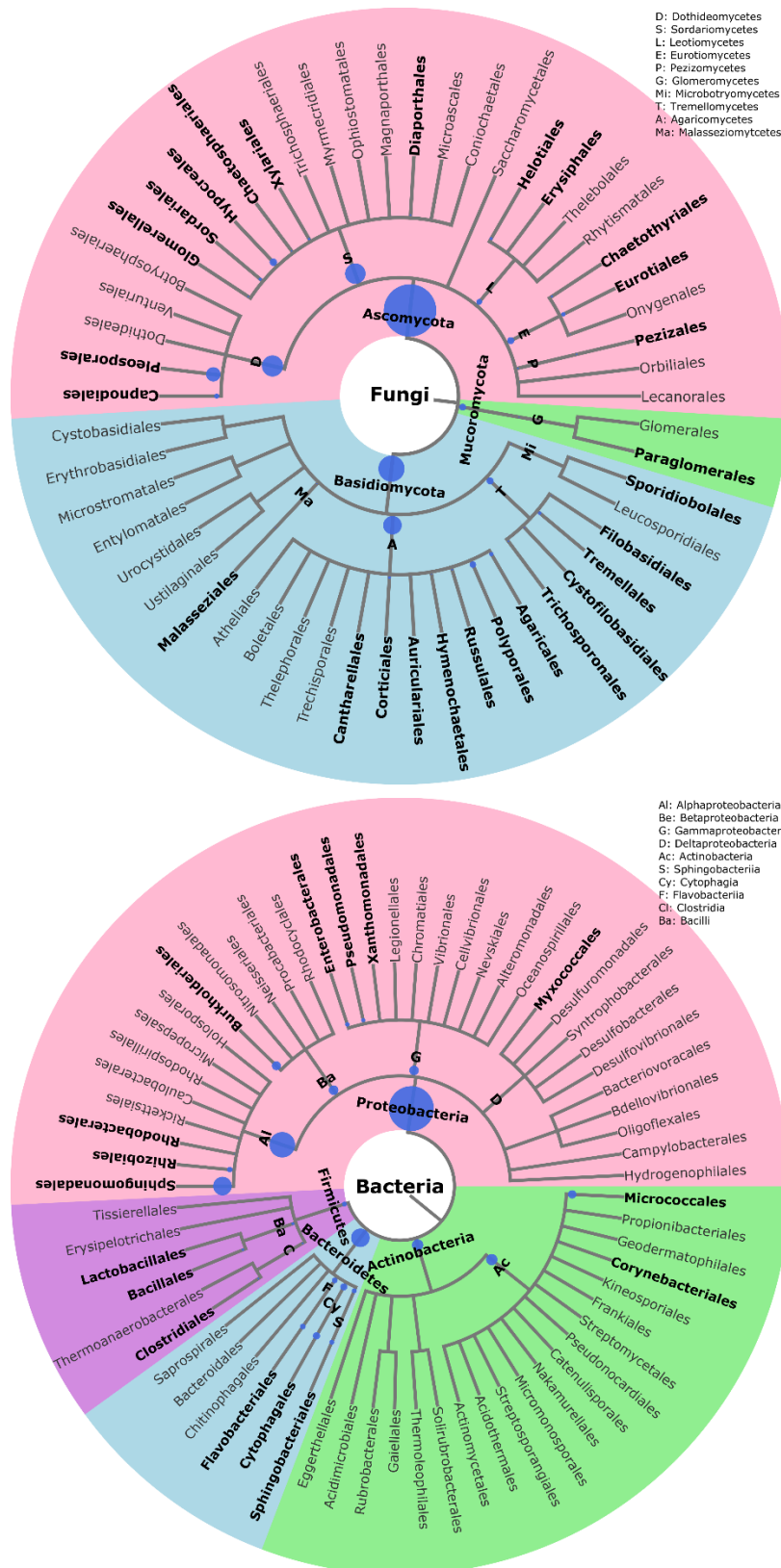
332 Statistical assignment of airborne PM₁₀ fungal MOTUs at different taxonomic levels reveals 3 phyla, 17 classes,
 333 58 orders and 160 families (Fig. 3). Interestingly, fungal MOTUs are dominated by two common phyla:
 334 Ascomycota (accounting for an average of $76 \pm 20.4\%$ (average \pm SD)) of fungal sequences across all air samples,
 335 followed by Basidiomycota ($23.9 \pm 20.4\%$). The remaining sequences correspond to Mucoromycota ($< 0.01\%$) and
 336 to unclassified sequences (approximately 0.03%). As evidenced in Fig. 3, the predominant ($> 1\%$) fungal classes
 337 are Dothideomycetes (70.0%), followed by Agaricomycetes (16.0%), Tremellomycetes (5.0%), Sordariomycetes
 338 (2.6%), Microbotryomycetes (2.2%), Leotiomycetes (1.8%) and Eurotiomycetes (1.4%). The predominant orders
 339 include Pleosporales (35.5 %) and Capnodiales (34.4 %), which belong to Ascomycota. Likewise, the dominant
 340 orders in Basidiomycota are Polyporales (7.5%), followed by Russulales (4.2%), Tremellales (2.8%),
 341 Hymenochaetales (2.6%) and Sporidiobolales (2.2%). At the genus level, about 327 taxa are characterized across
 342 all air samples, among which *Cladosporium* (32.9%), *Alternaria* (15.0%), *Epicoccum* (15.0%), *Peniophora*
 343 (2.7%), *Sporobolomyces* (2.2 %), *Phlebia* (2.0%) and *Pyrenophora* (1.9 %) are the most abundant communities.

344 3.3.2. Bacterial communities

345 For bacterial communities, the BactO2 marker allowed identifying 17 phyla, 43 classes, 91 orders and 182 families
 346 (Fig. 3). Predominant phyla include Proteobacteria ($55.3 \pm 8.6\%$), followed by Bacteroidetes ($22.1 \pm 4.1\%$),
 347 Actinobacteria ($14.2 \pm 2.2\%$), Firmicutes ($6 \pm 5.9\%$), with less than 1.8 % of the total bacterial sequence reads being
 348 unclassified. At the class level, the predominant bacteria are Alphaproteobacteria (29.4%), Actinobacteria (13.8%),
 349 Gammaproteobacteria (12.1%), Betaproteobacteria (11.4%), Cytophagia (8.3%), Flavobacteriia (6.3%),

350 Sphingobacteria (5.9%), Bacilli (3.5%) and Clostridia (2.2%). As many as 392 genera were detected in all aerosol
351 samples, although many sequences (22.8%) could not be taxonomically assigned at the genus level. The most
352 abundant (> 2%) genera are *Sphingomonas* (20.0%), followed by *Massilia* (8.4%), *Hymenobacter* (5.5%),
353 *Pseudomonas* (5.1%), *Pedobacter* (3.3%), *Flavobacterium* (2.8%), *Chryseobacterium* (2.8%), *Frigoribacterium*
354 (2.5%), and *Methylobacterium* (1.9%).

355



356

357 **Figure 3: Taxonomic and phylogenetic trees of fungal and bacterial community structure in PM₁₀ at the study site.**
 358 **Phylogenetic trees are analysed with the Environment for Tree Exploration (ETE3) package implemented in Python**
 359 **(Huerta-Cepas et al., 2016). The circle from inner to outer layer represents classification from kingdom to order**
 360 **successively. Further details on fungal and bacterial taxa at genus level are provided in Fig. S4. The node size represents**
 361 **the average relative abundance of taxa. Only nodes with relative abundance ≥ 1 are highlighted in bold.**

362 3.4. Relationship between airborne microbial community abundances and PM₁₀ SC species

363 The NMDS (non-metric multidimensional scaling) ordination exploring the temporal dynamics of microbial
364 community beta diversity among all PM₁₀ aerosol samples revealed significant temporal shifts of community
365 structure for both fungi and bacteria (Fig. 4).

366 An NMDS (two dimensions, stress = 0.15) based on fungal class-level compositions (Fig. 4A) results in three
367 distinct clusters of PM₁₀ samples. With one exception (A23), all air samples with higher SC concentration levels
368 (A5 to A20, see Table S2 and Fig. S1) are clustered together and are distinct from those with background levels
369 of atmospheric SC concentrations. This pattern is further confirmed with the analysis of similarity, which shows
370 a significant separation of clusters of samples (ANOSIM; $R = 0.31$, $p < 0.01$). As evidenced in Fig. 4A, this
371 difference is mainly explained by the NMDS1 axis, which results from the predominance of only a few class-level
372 fungi in PM₁₀ samples, including *Dothideomycetes*, *Tremellomycetes*, *Microbotryomycetes* and
373 *Exobasidiomycetes*. Vector fitting of chemical time series data to the NMDS ordination plot indicates that the latter
374 four fungal community assemblage best correlates with individual SC species. Mannitol ($R^2 = 0.37$, $p < 0.01$),
375 arabitol ($R^2 = 0.36$, $p < 0.01$), trehalose ($R^2 = 0.41$, $p < 0.01$), glucose ($R^2 = 0.33$, $p < 0.01$), xylitol ($R^2 = 0.45$, p
376 < 0.01), erythritol ($R^2 = 0.40$, $p < 0.01$) and inositol ($R^2 = 0.24$, $p = 0.01$) are significantly positively correlated to
377 the fungal assemblage ordination solution.

378 For bacterial phylum-level compositions (Fig. 4B), an NMDS ordination (two dimensions, stress = 0.07) analysis
379 differentiates the PM₁₀ samples into two distinct clusters according to their SC concentrations levels. All air
380 samples with higher SC concentration levels except two (A23 and A24) are clustered separately from those with
381 ambient background concentration levels. ANOSIM analysis ($R = 0.69$, $p < 0.01$) further confirms the significant
382 difference between the two clusters of samples. Proteobacteria constitutes the most dominant bacterial phylum
383 during the SC peak over the sampling period. Interestingly, changes in individual SC profiles are significantly
384 correlated with bacterial community temporal shifts (Fig. 4B). Mannitol ($R^2 = 0.25$, $p < 0.01$), arabitol ($R^2 = 0.24$,
385 $p < 0.01$), trehalose ($R^2 = 0.32$, $p < 0.01$), glucose ($R^2 = 0.32$, $p < 0.01$), xylitol ($R^2 = 0.38$, $p < 0.01$) and erythritol
386 ($R^2 = 0.27$, $p < 0.01$) are mainly positively correlated to the bacterial community dissimilarity.

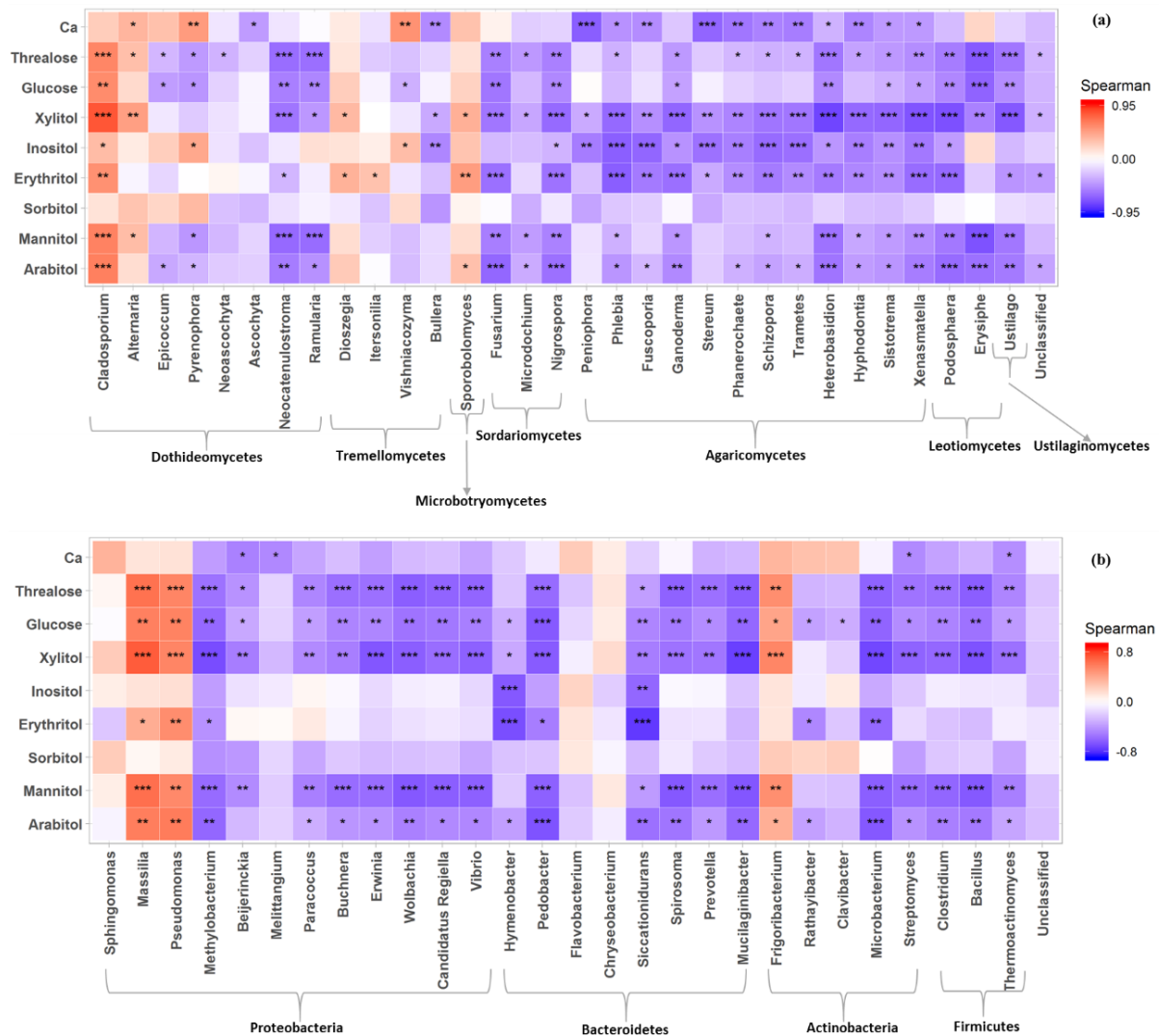
387 Given the distinct clustering patterns of airborne PM₁₀ microbial beta diversity structures according to SC
388 concentration levels, a Pearson's rank correlation analysis has been performed to further examine the relationships
389 between individual SC profiles and airborne microbial community abundance at phylum or class levels. This
390 analysis reveals that for class-level fungi, the abundances of *Dothideomycetes*, *Tremellomycetes* and
391 *Microbotryomycetes* are highly positively correlated ($p < 0.05$) to the temporal evolutions of the individual SC
392 species concentration levels (Fig. S5A). Likewise, ambient SC species concentration levels are significantly
393 correlated ($p < 0.05$) to the Proteobacteria phylum (Fig. S5B). To gain further insight into the airborne microbial
394 fingerprints associated with ambient SC species, correlation analyses were also performed at a finer taxonomic
395 level. These analyses show that the temporal dynamics of SC species primarily correlates best ($p < 0.05$) with the
396 *Cladosporium*, *Alternaria*, *Sporobolomyces* and *Dioszegia* fungal genera (Fig. 5A). Similarly, the time series of
397 SC species are primarily positively correlated ($p < 0.05$) with *Massilia*, *Pseudomonas*, *Frigoribacterium*, and to a
398 lesser degree (non-significant) with the *Sphingomonas* bacterial genus (Fig. 5B).



399 **Figure 4: Main airborne microbial communities associated with atmospheric concentrations of SC species. NMDS**
 400 **ordination plots are used to show relationship among time series of aerosol samples. The stress values indicate an**
 401 **adequate 2-dimensional picture of sample distribution. Ellipses represent 95% confidence intervals for the cluster**
 402 **centroid. NMDS analyses are performed directly on taxonomically assigned quality-filtered sequences tables at class**
 403 **and phylum level respectively for fungi (A) and bacteria (B). Ambient primary sugar concentration levels in PM₁₀**
 404 **appear to be highly influenced by the airborne microbial community structure and abundance. Similar results are**
 405 **obtained with taxonomically assigned MOTU tables, highlighting the robustness of our methodology.**
 406

407

408



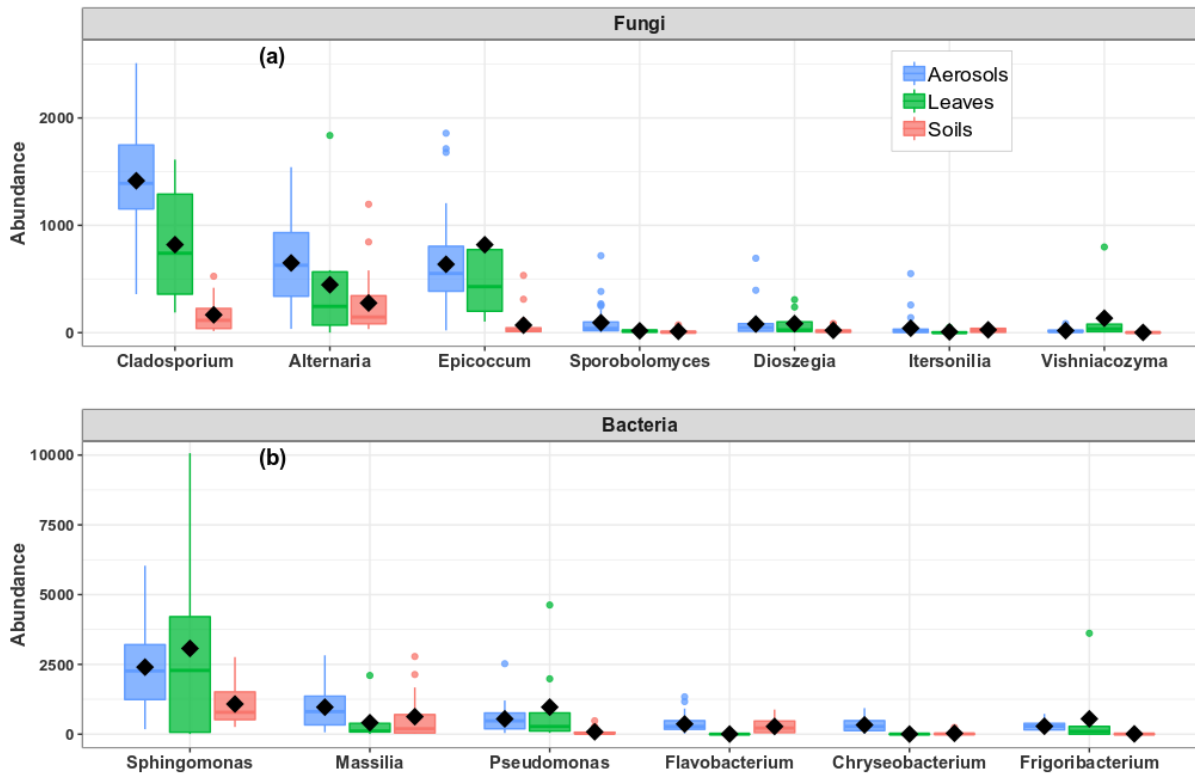
409

410 **Figure 5: Heatmap of Spearman's rank correlation between SCs and abundance of airborne communities at the study**
 411 **site. (A) Fungal and (B) bacterial genus, respectively. Only genera with relative abundance ≥ 1 are shown.**

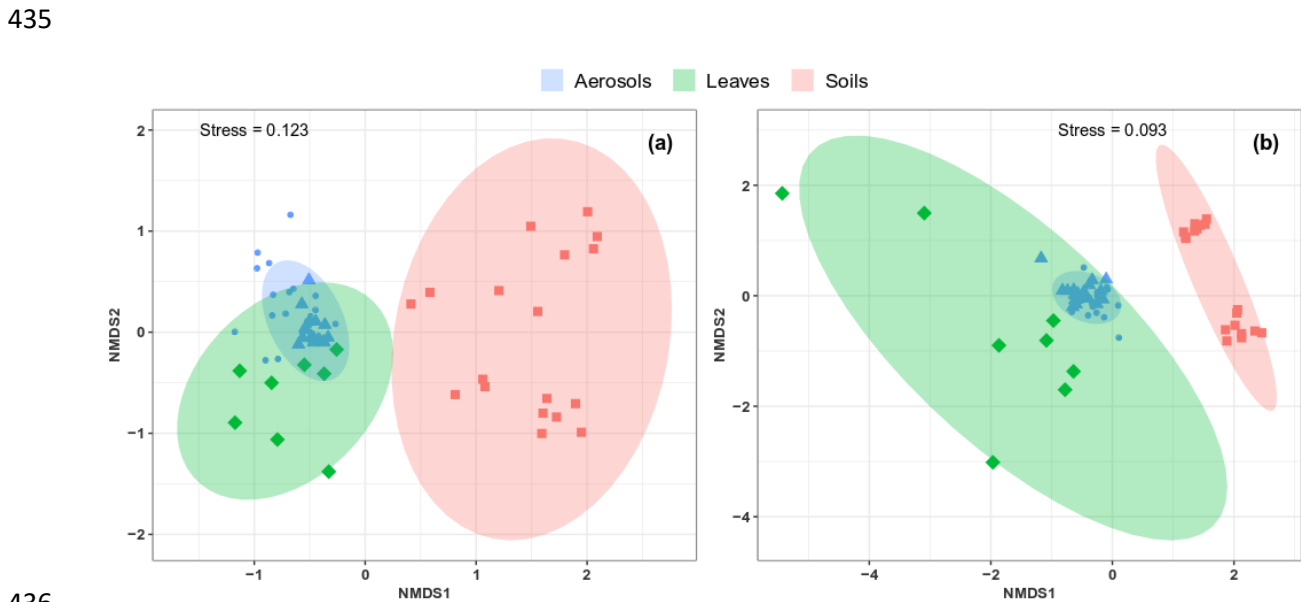
412 **3.5. Sources of airborne microbial communities at the study site**

413 As shown in Fig. 6, the airborne microbial genera most positively correlated with SC species are also distributed
 414 in the surrounding environmental samples of surface soils and leaves. In addition, microbial taxa of PM₁₀
 415 associated with SC species are generally more abundant in the leaves than in the topsoil samples (Fig. 5). In order
 416 to further explore and visualize the similarity of species compositions across local environment types, we
 417 conducted an NMDS ordination analysis (Fig. 6). As evidenced in Fig. 6, the beta diversities of fungal and bacterial
 418 MOTUs are more similar within the same habitat (PM₁₀, plant, or soil) and are grouped across habitats as expected.
 419 Interestingly, the beta diversities of fungal and bacterial MOTUs in leaf samples and those in airborne PM₁₀ are
 420 generally not readily distinguishable, with similarity becoming more prominent during atmospheric peaks of SC
 421 concentration levels (Fig. 6). However, the overall beta diversities in airborne PM₁₀ and in leaf samples are
 422 significantly different from those from topsoil samples (ANOSIM, R = 0.89 and 0.80, p < 0.01 for fungal and
 423 bacterial communities, respectively), without any overlap regardless of whether or not harvesting activities are
 424 performed around the sampling site.

425 This observation is also confirmed by an unsupervised hierarchical cluster analysis, which reveals a pattern similar
 426 to that observed in the NMDS ordination, where taxa from leaf samples and airborne PM₁₀ are clustered together,
 427 regardless of whether ambient concentration levels of SC peaked or not, and they are clustered separately from
 428 those of topsoil samples (Fig. S7).



429
 430 **Figure 6: Abundance of SC species-associated microbial taxa. (A) Fungal and (B) bacterial genera in the airborne PM₁₀**
 431 **samples and surrounding environmental samples. Black markers inside each box indicate the mean abundance value,**
 432 **while the top, middle, and bottom lines of the box represent the 75th, median, and 25th percentile, respectively. The**
 433 **whiskers at the top and bottom of the box extend from the 95th to the 5th percent. Data were rarefied at the same**
 434 **minimum sequencing depth.**



436
 437 **Figure 7: Compositional comparison of sample types in a NMDS scaling ordination. NDMS plots are constructed from**
 438 **a Horn distance matrix of MOTUs abundances for fungi (A) and bacteria (B), respectively. Data sets are rarefied at the**
 439 **same sequencing depth. The stress values indicate an adequate two-dimensional picture of sample distribution. Ellipses**
 440 **represent 95% confidence intervals for the cluster centroids. Circular and triangular shapes highlight air PM₁₀ samples**
 441 **respectively with background and peak SC concentrations.**

442 4. Discussion

443 Very few studies exist about the interactions between air microbiome and PM chemical profiles (Cao et al., 2014;
444 Elbert et al., 2007). In this study, we used a comprehensive multidisciplinary approach to produce for the first time
445 airborne microbial fingerprints associated with SC species in PM₁₀ and to identify the dominant sources of SCs in
446 a continental rural area extensively cultivated.

447 4.1. SCs as a major source of organic matter in PM₁₀

448 SC species have recently been reported to be ubiquitous in PM₁₀ collected in several areas in France (Golly et al.,
449 2018; Samaké et al., 2019b). In this study, the total SC presented an average concentration of $259.8 \pm 253.8 \text{ ng m}^{-3}$
450 ³, with a range of 26.6 to 1,679.5 ng m⁻³ in all air samples. These concentration values are on average five times
451 higher than those typically observed in urban areas in France (average values during summer $48.5 \pm 43.6 \text{ ng.m}^{-3}$)
452 (Golly et al., 2018; Samaké et al., 2019a, 2019b). However, these concentration levels are in agreement with a
453 previous study conducted in a similar environment, i.e., continental rural sites located in large crop fields (Yan et
454 al., 2019).

455 The total concentrations of SC quantified in the atmospheric PM₁₀ over our study site accounted for 0.8 to 13.5%
456 of the daily OM mass. This is remarkable considering that less than 20% of total particulate OM mass can generally
457 be identified at the molecular level. Hence, our results for a nine week-long period indicate that SC could be a
458 major identified molecular fraction of OM for agricultural areas during summer, in agreement with several
459 previous studies conducted worldwide (Jia et al., 2010b; Verma et al., 2018; Yan et al., 2019). Further, it has been
460 shown (Samaké et al., 2019a) that the identified polyols most probably represent only a small fraction of the
461 emission flux from this PBOA source, and that a large fraction of the co-emitted organic material remains
462 unknown. Hence, the PBOA source can potentially represent, for part of the year, a major source of atmospheric
463 OM unaccounted for in CTM models.

464 4.2. Composition of airborne fungal and bacterial communities

465 In this study, 597 (39-132 MOTUs per sample) and 944 (31-129 MOTUs per sample) MOTUs were obtained for
466 the fungi and bacteria libraries, respectively, reflecting the high richness of airborne microbial communities
467 associated with ambient PM₁₀ in a rural agricultural zone in France. Airborne fungi were dominated by
468 Ascomycota (AMC) followed by Basidiomycota (BMC) phyla, consistent with the natural feature of many
469 Ascomycota, whose single-celled or hyphal forms are fairly small to be rapidly aerosolized, in contrast to many
470 Basidiomycota that are typically too large to be easily aerosolized (Moore et al., 2011; Womack et al., 2015).
471 Many members of AMC and BMC are well known to actively eject ascospores and basidiospores as well as
472 aqueous jets and droplets containing a mixture of carbohydrates and inorganic solutes into the atmosphere (Elbert
473 et al., 2007; Womack et al., 2015). The prevalence of Ascomycota and Basidiomycota is consistent with results
474 from previous studies also indicating that the Dikarya subkingdom (Ascomycota and Basidiomycota) represents
475 about 98% of known species in the biological Kingdom of Eumycota (i.e., fungi) in atmosphere (Elbert et al.,
476 2007; James et al., 2006; Womack et al., 2015; Xu et al., 2017)

477 Airborne bacteria in this study belonged mainly to the Proteobacteria, Bacteroidetes, Actinobacteria and
478 Firmicutes phyla, consistent with previous studies (Liu et al., 2019; Maron et al., 2005; Wei et al., 2019b). Gram-
479 negative Proteobacteria constitute a major taxonomic group among prokaryotes (Itävaara et al., 2016; Yadav et
480 al., 2018), which includes bacterial taxa very diverse and important in agriculture, capable of fixing nitrogen in
481 symbiosis with plants (Itävaara et al., 2016; Yadav et al., 2018). Proteobacteria can survive under conditions with
482 very low nutrient content, which explains their atmospheric versatility (Itävaara et al., 2016; Yadav et al., 2018).
483 These results are similar to those observed in previous studies conducted in different environments around the
484 world, where Proteobacteria, Actinobacteria and Firmicutes have also been reported as dominant bacterial phyla
485 (Liu et al., 2019; Maron et al., 2005; Wei et al., 2019a). In particular, the most frequent gram-negative
486 (Proteobacteria and Bacteroidetes) and gram-positive (Actinobacteria and Firmicutes) bacteria, and filamentous
487 fungi (Ascomycota and Basidiomycota) have been previously linked to raw straw handling activities. For instance,
488 it has been suggested that straw combustion during agricultural activities could be a major source of airborne
489 microorganisms in PM_{2.5} at the northern plains of China (Wei et al., 2019a, 2019b). However, in our study, SC
490 species are not correlated ($R = -0.09$, $p = 0.46$; Fig. S7) with levoglucosan during the campaign period, confirming
491 that biomass burning is not an important source of airborne microbial taxa associated with SCs in our PM₁₀ series.

492 Bubble bursting associated with sea spray could also potentially be a source of bacteria, fungi and water-soluble
493 organic species, along with sea salts, to PM₁₀ (Prather et al., 2013; Zhu et al., 2015). However, SC species were
494 not found to be significantly related to Cl⁻ (R = -0.14, p = 0.28) or Na⁺ (R = -0.18, p = 0.16), which are two
495 inorganic tracers typical of marine sources; nor correlated with methanesulfonic acid (R = -0.05, p = 0.69), a well-
496 known tracer of biogenic marine activity (Arndt et al., 2017; Gaston et al., 2010). It therefore seems unlikely that
497 the sources of SCs from marine environments were significant at this site. This point is further discussed in Sect.
498 4.4.

499 **4.3. Atmospheric concentration levels of SC species in PM₁₀ are associated with the abundance of few** 500 **specific airborne taxa of fungi and bacteria**

501 SCs are widely produced in large quantities by many microorganisms to cope with environmental stress conditions
502 (Medeiros et al., 2006). SC species are known to accumulate at high concentrations in microorganisms at low
503 water availability to reduce intracellular water activity and prevent enzyme inhibition due to dehydration
504 (Hryniewicz et al., 2010). In addition, temporal dynamics of ambient polyols concentrations have been suggested
505 as an indicator to follow the general seasonal trend in airborne fungal spore counts (Bauer et al., 2008; Gosselin et
506 al., 2016). Although this strategy has allowed introducing conversion ratios between specific polyols species (i.e.,
507 arabitol and mannitol) and airborne fungal spores in general (Bauer et al., 2008), the structure of the airborne
508 microbial community associated with SC species has not yet been studied. Our results provide culture-independent
509 evidence that the airborne microbiome structure and the combined bacterial and fungal communities largely
510 determine the SC species concentration levels in PM₁₀.

511 Temporal fluctuations in the abundance of only few specific fungal and bacterial genera reflect the temporal
512 dynamics of ambient SC concentrations. For fungi, genera that show a significant positive correlation (p < 0.05)
513 with SC species includes *Cladosporium*, *Alternaria*, *Sporobolomyces* and *Dioszegia*. *Cladosporium* and
514 *Alternaria*, are fungal genera that contribute on average to 47.9% of total fungal sequence reads in our air samples
515 series. These are asexual fungal genera that produce spores by dry-discharge mechanisms wherein spores are
516 detached from their parent colonies and easily dispersed by the ambient air flow or other external forces (e.g.,
517 raindrops, elevated temperature, etc.), as opposed to actively discharged spores with liquid jets or droplets into the
518 air (Elbert et al., 2007; Wei et al., 2019b; Womack et al., 2015). Our results are consistent with the well-known
519 seasonal behavior of airborne fungal spores, with levels of *Cladosporium* and *Alternaria* which have been shown
520 to reach their maximum from early to midsummer in a rural agricultural area of Portugal (Oliveira et al., 2009).

521 Similarly, bacterial genera positively correlated with SC species are *Massilia*, *Pseudomonas*, *Frigoribacterium*,
522 and *Sphingomonas*. Although it is the prevalent bacterial genus at the study site, *Sphingomonas* is indeed not
523 significantly positively correlated with SC species. The genus *Sphingomonas* is well-known to include numerous
524 metabolically versatile species capable of using carbon compounds usually present in the atmosphere (Cáliz et al.,
525 2018). The atmospheric abundance of species affiliated with *Massilia* has already been linked to the change in the
526 stage of plant development (Ofek et al., 2012), which can be attributed to the capacity of *Massilia* to promote plant
527 growth, through the production of indole acetic acid (Kuffner et al., 2010), or siderophores (Hryniewicz et al.,
528 2010), and to be antagonist towards *Phytophthora infestans* (Weinert et al., 2010).

529 As far as we know, this is the first study evaluating microbial fingerprints with SC species in atmospheric PM,
530 hence it is not possible to compare our correlation results with that of previous works. However, it has already
531 been suggested that types and quantities of SC species produced by fungi under culture conditions are specific to
532 microbial species and external conditions such as carbon source, drought and heat, etc. (Hryniewicz et al., 2010).
533 In future studies, we intend to apply a culture-dependent method to directly characterize the SC contents of some
534 species amongst the dominant microbial taxa identified in this study after growth under several laboratory
535 chambers reproducing controlled environmental conditions in terms of temperature, water vapor or carbon sources.

536 **4.4. Local vegetation as major source of airborne microbial taxa of PM₁₀ associated with SC species**

537 There are still many challenging questions on the emission processes leading to fungi and bacteria being introduced
538 into the atmosphere, together with their chemical components. In particular, the potential influence of soil and
539 vegetation and their respective roles in structuring airborne microbial communities is still debated
540 (Lymperopoulou et al., 2016; Rathnayake et al., 2016; Womack et al., 2015), especially since this knowledge is

541 particularly essential for the precise modeling of PBOA emissions processes to the atmosphere within Chemical
542 Transport Models.

543 Characterization of the temporal dynamics of SC species concentrations could provide important information on
544 PBOA sources in terms of composition, environmental drivers and impacts. The results obtained over a nine week-
545 period of daily PM₁₀ SC measurements clearly show that the temporal dynamics of sorbitol ($R= 0.59$, $p < 0.001$)
546 and inositol ($R= 0.64$, $p < 0.001$) are well correlated linearly with that of calcium, a typical inorganic water-soluble
547 ion from crustal material. This indicates a common atmospheric origin for these chemicals. Sorbitol and inositol
548 are well-known reduced sugars that serve as carbon source for microorganisms when other carbon sources are
549 limited (Ng et al., 2018; Xue et al., 2010). In microorganisms, sorbitol and inositol are mainly produced by the
550 reduction of intracellular glucose by aldose reductase in the cytoplasm (Ng et al., 2018; Welsh, 2000; Xue et al.,
551 2010). Moreover, significant concentrations of both sorbitol and inositol have already been measured in surface
552 soil samples from five cultivated fields in the San Joaquin Valley, USA (Jia et al., 2010b; Medeiros et al., 2006).
553 Therefore, sorbitol and inositol are most likely associated with microorganisms from soil resuspension.

554 With the exception of sorbitol and inositol, all other SC species measured in air samples at our sampling site are
555 strongly correlated with each other, indicating a common origin. Daily calcium concentration peaks are not
556 systematically associated with those of these other SC species. Interestingly, the highest atmospheric levels of
557 these SC species occurred on August 8th 2017, coinciding well with daily harvesting activities around the site. This
558 is also consistent with a multi-year monitoring of the dominant SCs in PM₁₀ at this site, where ambient SCs showed
559 a clear seasonal trend with higher values recorded in early August and in good agreement with harvesting activities
560 around the study area every year from 2012 to 2017 (Samaké et al., 2019a). This suggests that the processes
561 responsible for the dynamics of atmospheric concentrations of SCs are replicated annually and most likely
562 effective over large areas of field crop (Golly et al., 2018; Samaké et al., 2019a). Interestingly, glucose—the most
563 common monosaccharide present in vascular plants and microorganisms— has already been proposed as
564 molecular indicator of biota emitted into the atmosphere by vascular plants and/or by the resuspension of soil from
565 agricultural land (Jia et al., 2010b; Pietrogrande et al., 2014). Therefore, all other SC species measured in our series
566 can be considered to be most likely the result of the mechanical resuspension of crop residues (e.g., leaf debris)
567 and microorganisms attached to them. Other confirmations of this interpretation stem from the excellent daily co-
568 variations observed in the PM₁₀ between SC species levels and ambient cellulose, widely considered as a reliable
569 indicator of the plant debris source in PM studies (Bozzetti et al., 2016; Hiranuma et al., 2019).

570 Microbial abundance and community structure in samples from the surrounding environment can provide further
571 useful information on sources apportionment and importance. Our data indicates that the airborne microbial genera
572 most positively correlated to SC species are also distributed in surrounding environmental samples from both
573 surface soils and leaves, suggesting a dominant influence of the local environments for microbial taxa associated
574 with SC species, as opposed to long-range transport. This observation makes sense since actively discharged
575 ascospores and basidiospores are generally relatively large airborne particles with short atmospheric residence
576 time (Elbert et al., 2007; Womack et al., 2015), limiting the possibilities of long-range dissemination. Accordingly,
577 the majority of previous studies investigating the potential sources of air microbes identified the local surface
578 environments (e.g., leaves, soils, etc.) to have more important effects on airborne microbiome structure in field
579 crop areas (Bowers et al., 2011; Wei et al., 2019b; Womack et al., 2015). This is all the more the case in our study,
580 with homogeneous crop activities for 10's to 100's of km around the site.

581 In the present study, microbial diversity and richness observed in the surface soils are generally higher than those
582 in leaf surfaces. Microbial taxa most positively correlated with PM₁₀ SC species are generally more abundant in
583 leaf than in topsoil samples. These results were unexpected and show the possible importance of leaf surfaces in
584 structuring the airborne taxa associated with SC species. Considering the general grouping of leaf samples and
585 airborne PM₁₀ regardless of harvesting activities around the study site in addition to the separate assemblies of
586 rarefied MOTUs in airborne PM₁₀ and topsoil samples, it can be argued that aerial parts of plants are the major
587 source of microbial taxa associated with SC species. Such observation is most likely related to increased vegetative
588 surface (e.g., leaves) in summer that provides sufficient nutrient resources for microbial growth (Rathnayake et
589 al., 2016). By reviewing previous studies, *Alternaria* and *Epicocum*, which made 30% of total fungal sequence
590 reads in all air samples in this study, have been shown to be common saprobes or weak pathogens of leaf surfaces
591 (Andersen et al., 2009). Similarly, *Cladosporium*, which accounted for 32.9% of total fungal genera in all air
592 samples, have also been shown to be a common saprotrophic fungi inhabiting in decayed tree or plant debris (Wei
593 et al., 2019b). The high relative abundance of *Sphingomonas* and *Massilia*, accounting for 28.4% of total bacterial

594 genera in all air samples, is also noticeable. These two phyllosphere inhabiting bacterial genera are well-known
595 for their plant protective potential against phytopathogens (Aydogan et al., 2018; Rastogi et al., 2013).

596 Altogether, these observations support our interpretation that leaves are the major direct source of airborne fungi
597 and bacteria during the summer months at this site of large agricultural activities. Endophytes and epiphytes can
598 be dispersed in the air and transported vertically as particles by the air currents, much faster and more widely than
599 by other mechanisms, such as direct dissemination from surface soil, which is generally controlled by soil moisture
600 (Jocteur Monrozier et al., 1993). The most wind-dispersible soil constituents are indeed the smallest soil particles
601 (i.e. clay-size fraction), which contain the largest number of microorganisms (Jocteur Monrozier et al., 1993) and
602 can only be released into the atmosphere under conditions of prolonged drought. This interpretation is also
603 consistent with previous studies (Bowers et al., 2011; Liu et al., 2019; Lymperopoulou et al., 2016; Mhuireach et
604 al., 2016), which also show the extent to which endophytes and epiphytes can serve as quantitatively important
605 sources of airborne microbes during summertime when vegetation density is highest. For example,
606 Lymperopoulou et al. (2016) observed that bacteria and fungi suspended in the air are generally two to more than
607 ten times more abundant in air that passed over 50 m of vegetated surface than that is immediately upwind of the
608 same vegetated surface. However, the relatively abundance of taxa associated with SCs in surface soils in this
609 study could also be indicative of a feedback loop in which the soil may serve as sources of microbial endophytes
610 and epiphytes for plants while the local vegetation in turns may serve as sources and sinks of microbes for local
611 soils during leaf senescence.

612 5. Conclusion

613 Primary biogenic organic aerosols (PBOA) affects human health, climate, agriculture, etc. However, the details of
614 microbial communities associated with the temporal and spatial variations in atmospheric concentrations of SC,
615 tracers of PBOA, remain unknown. The present study aimed at identifying the airborne fungi and bacteria
616 associated with SC species in PM₁₀ and their major sources in the surrounding environment (soils and vegetation).
617 To that end, we combined high-throughput sequencing of bacteria and fungi with detailed physicochemical
618 characterization of PM₁₀ soils and leaf samples collected at a continental rural background site located in a large
619 agricultural area in France.

620 The main results demonstrate that the identified SC species are a major contributor of OM in summer, accounting
621 together for 0.8 to 13.5% of OM mass in air. The atmospheric concentration peaks of SC are coincident the daily
622 harvest activities around the sampling site, pointing towards direct resuspension of biological materials, i.e. crop
623 residues and associated microbiota as an important source of SC in our PM₁₀ series. Furthermore, we have also
624 discovered that the temporal evolutions of SC in PM₁₀ are associated with the abundance of only few specific
625 airborne fungi and bacteria taxa. These microbial taxa are significantly enhanced in the surrounding environmental
626 samples of leaves over surface soils. Finally, the excellent correlation of SC species and cellulose, a marker of
627 plant materials, implies that local vegetation is likely the most important source of fungi and bacteria taxa
628 associated with SC in PM₁₀ at rural locations directly influenced by agricultural activities in France.

629 Our findings is a first step in the understanding of the processes leading to the emission of these important chemical
630 species and large OM fraction of PM in the atmosphere, and to the parametrization of these processes for their
631 introduction in CTM models. They could also be used for planning efforts to reduce both the PBOA source
632 strengths and the spreading of airborne microbial and derivative allergens such as endotoxins, mycotoxins, etc.
633 However, it remains to investigate how-well different climate patterns and sampling site specificities, in terms of
634 land use and vegetation cover, could affect our main conclusions.

635

636 **Data and materials availability:** The sequencing data files are available from the DRYAD repository
637 (doi:10.5061/dryad.2fqz612m4). All relevant chemical and environmental data sets are archived at the IGE
638 (Institut des Géosciences de l'Environnement), and are available upon request from the co-author (Jean-Luc
639 Jaffrezo).

640 **Competing interests:** The authors declare that they have no competing interests.

641 **Author contributions:** J.-L.J., J-M-F.M., G.U. supervised the thesis of A.S. and J.-L.J., J.M.F.-M., G.U and A.S.
642 designed the research project. P.T. gives advice for soils and leaves sampling. S.C. supervised the sample
643 collections and provided the agricultural activity records. V.J. developed the analytical techniques for SC species
644 and cellulose measurements. A.S. and A.B. performed the experiments. A.B. performed the bioinformatic
645 analyses. A.S. performed statistical analyses and wrote the original manuscript draft. S.W. produced the circular
646 phylogenetic trees. All authors reviewed and edited the final manuscript.

647 **Acknowledgements:** We acknowledge the work of many engineers in the lab at the Institut des Géosciences de
648 l'Environnement for the analyses (Anthony Vella, Vincent Lucaire). The authors would like to kindly thank the
649 dedicated efforts of many other people at the sampling site and in the laboratories for collecting and analyzing the
650 samples.

651 **Financial support:** The PhD of Abdoulaye Samaké is funded by the Government of Mali. We gratefully
652 acknowledge the LEFE-CHAT and EC2CO programs of the CNRS for financial supports of the CAREMBIOS
653 multidisciplinary project, with ADEME funding. Chemical and microbiological analytical aspects were supported
654 at IGE by the Air-O-Sol and MOME platforms, respectively, within Labex OSUG@2020 (ANR10 LABX56).

655 **References**

- 656 Amato, P., Brisebois, E., Draghi, M., Duchaine, C., Fröhlich-Nowoisky, J., Huffman, J. A., Mainelis, G., Robine,
657 E., and Thibaudon, M.: Main biological aerosols, specificities, abundance, and diversity, in *Microbiology of*
658 *Aerosols*, pp. 1–21, John Wiley & Sons, Ltd., <https://doi.org/10.1002/9781119132318>, 2017.
- 659 Andersen, G. L., Frisch, A. S., Kellogg, C. A., Levetin, E., Lighthart, B., and Paterno, D.: Aeromicrobiology/air
660 quality, in *Encyclopedia of Microbiology (Third Edition)*, pp. 11–26, Academic Press, Oxford., doi:
661 10.1016/B978-012373944-5.00166-8, 2009.
- 662 Arndt, J., Sciare, J., Mallet, M., Roberts, G. C., Marchand, N., Sartelet, K., Sellegri, K., Dulac, F., Healy, R. M.,
663 and Wenger, J. C.: Sources and mixing state of summertime background aerosol in the north-western
664 Mediterranean basin, *Atmos. Chem. Phys.*, 17(11), 6975–7001, doi:10.5194/acp-17-6975-2017, 2017.
- 665 Aydogan, E. L., Moser, G., Müller, C., Kämpfer, P., and Glaeser, S. P.: Long-term warming shifts the composition
666 of bacterial communities in the phyllosphere of galium album in a permanent grassland field-experiment, *Front.*
667 *Microbiol.*, 9, 144, doi:10.3389/fmicb.2018.00144, 2018.
- 668 Barbaro, E., Kirchgeorg, T., Zangrando, R., Vecchiato, M., Piazza, R., Barbante, C., and Gambaro, A.: Sugars in
669 Antarctic aerosol, *Atmos. Environ.*, 118, 135–144, doi:10.1016/j.atmosenv.2015.07.047, 2015.
- 670 Bauer, H., Claeys, M., Vermeylen, R., Schueller, E., Weinke, G., Berger, A., and Puxbaum, H.: Arabitol and
671 mannitol as tracers for the quantification of airborne fungal spores, *Atmos. Environ.*, 42(3), 588–593,
672 doi:10.1016/j.atmosenv.2007.10.013, 2008.
- 673 Boucher, O., Randall, D., Artaxo, P., Bretherton, C., Feingold, G., Forster, P., Kerminen, V.-M., Kondo, Y., Liao,
674 H., and Lohmann, U.: Clouds and aerosols, in *Climate change 2013: the physical science basis. Contribution of*
675 *Working Group I to the Fifth Assessment Report of the Intergovernmental Panel on Climate Change*, pp. 571–
676 657, Cambridge University Press., doi:10.1017/CBO9781107415324.016, 2013.
- 677 Bougouffa, S., Radovanovic, A., Essack, M., and Bajic, V. B.: DEOP: a database on osmoprotectants and
678 associated pathways, *Database*, 2014, doi:10.1093/database/bau100, 2014.
- 679 Bowers, R. M., Sullivan, A. P., Costello, E. K., Collett, J. L., Knight, R., and Fiereri, N.: Sources of bacteria in
680 outdoor air across cities in the Midwestern United States., *Appl. Environ. Microbiol.*, 77(18), 6350–6356, doi:
681 0.1128/AEM.05498-11, 2011.
- 682 Boyer, F., Mercier, C., Bonin, A., Le Bras, Y., Taberlet, P., and Coissac, E.: OBITOOLS : a UNIX -inspired
683 software package for DNA metabarcoding, *Mol. Ecol. Resour.*, 16(1), 176–182, doi:10.1111/1755-0998.12428,
684 2016.
- 685 Bozzetti, C., Daellenbach, K. R., Hueglin, C., Fermo, P., Sciare, J., Kasper-Giebl, A., Mazar, Y., Abbaszade, G.,
686 El Kazzi, M., Gonzalez, R., Shuster-Meiseles, T., Flasch, M., Wolf, R., Křepelová, A., Canonaco, F., Schnelle-
687 Kreis, J., Slowik, J. G., Zimmermann, R., Rudich, Y., Baltensperger, U., El Haddad, I., and Prévôt, A. S. H.: Size-
688 resolved identification, characterization, and quantification of primary biological organic aerosol at a European
689 rural site, *Environ. Sci. Technol.*, 50(7), 3425–3434, doi:10.1021/acs.est.5b05960, 2016.
- 690 Cáliz, J., Triadó-Margarit, X., Camarero, L., and Casamayor, E. O.: A long-term survey unveils strong seasonal
691 patterns in the airborne microbiome coupled to general and regional atmospheric circulations, *Proc. Natl. Acad.*
692 *Sci.*, 115(48), 12229, doi:10.1073/pnas.1812826115, 2018.

693 Cao, C., Jiang, W., Wang, B., Fang, J., Lang, J., Tian, G., Jiang, J., and Zhu, T. F.: Inhalable microorganisms in
694 Beijing's PM_{2.5} and PM₁₀ pollutants during a severe smog event, *Environ. Sci. Technol.*, 48(3), 1499–1507,
695 doi:10.1021/es4048472, 2014.

696 Cavalli, F., Viana, M., Yttri, K. E., Genberg, J., and Putaud, J.-P.: Toward a standardised thermal-optical protocol
697 for measuring atmospheric organic and elemental carbon: the EUSAAR protocol, *Atmos. Meas. Tech.*, 3(1), 79–
698 89, doi:10.5194/amt-3-79-2010, 2010.

699 China, S., Burrows, S. M., Wang, B., Harder, T. H., Weis, J., Tanarhte, M., Rizzo, L. V., Brito, J., Cirino, G. G.,
700 Ma, P.-L., Cliff, J., Artaxo, P., Gilles, M. K., and Laskin, A.: Fungal spores as a source of sodium salt particles in
701 the Amazon basin, *Nat. Commun.*, 9(1), doi:10.1038/s41467-018-07066-4, 2018.

702 Ciarelli, G., Aksoyoglu, S., Crippa, M., Jimenez, J.-L., Nemitz, E., Sellegri, K., Äijälä, M., Carbone, S., Mohr, C.,
703 O'Dowd, C., Poulain, L., Baltensperger, U., and Prévôt, A. S. H.: Evaluation of European air quality modelled by
704 CAMx including the volatility basis set scheme, *Atmos. Chem. Phys.*, 16(16), 10313–10332, doi:10.5194/acp-16-
705 10313-2016, 2016.

706 Coz, E., Artúñano, B., Clark, L. M., Hernandez, M., Robinson, A. L., Casuccio, G. S., Lersch, T. L., and Pandis,
707 S. N.: Characterization of fine primary biogenic organic aerosol in an urban area in the northeastern United States,
708 *Atmos. Environ.*, 44(32), 3952–3962, doi:10.1016/j.atmosenv.2010.07.007, 2010.

709 Dommergue, A., Amato, P., Tignat-Perrier, R., Magand, O., Thollot, A., Joly, M., Bouvier, L., Sellegri, K., Vogel,
710 T., Sonke, J. E., Jaffrezo, J.-L., Andrade, M., Moreno, I., Labuschagne, C., Martin, L., Zhang, Q., and Larose, C.:
711 Methods to investigate the global atmospheric microbiome, *Front. Microbiol.*, 10, 243,
712 doi:10.3389/fmicb.2019.00243, 2019.

713 Elbert, W., Taylor, P. E., Andreae, M. O., and Pöschl, U.: Contribution of fungi to primary biogenic aerosols in
714 the atmosphere: wet and dry discharged spores, carbohydrates, and inorganic ions, *Atmos. Chem. Phys.*, 7(17),
715 4569–4588, doi:10.5194/acp-7-4569-2007, 2007.

716 Ficetola, G., Coissac, E., Zundel, S., Riaz, T., Shehzad, W., Bessière, J., Taberlet, P., and Pompanon, F.: An in
717 silico approach for the evaluation of DNA barcodes, *BMC Genomics*, 11(1), 434, doi:10.1186/1471-2164-11-434,
718 2010.

719 Fortenberry, C. F., Walker, M. J., Zhang, Y., Mitroo, D., Brune, W. H., and Williams, B. J.: Bulk and molecular-
720 level characterization of laboratory-aged biomass burning organic aerosol from oak leaf and heartwood fuels,
721 *Atmos. Chem. Phys.*, 18(3), 2199–2224, doi:10.5194/acp-18-2199-2018, 2018.

722 Fröhlich-Nowoisky, J., Kampf, C. J., Weber, B., Huffman, J. A., Pöhlker, C., Andreae, M. O., Lang-Yona, N.,
723 Burrows, S. M., Gunthe, S. S., Elbert, W., Su, H., Hoor, P., Thines, E., Hoffmann, T., Després, V. R., and Pöschl,
724 U.: Bioaerosols in the earth system: climate, health, and ecosystem interactions, *Atmos. Res.*, 182, 346–376,
725 doi:10.1016/j.atmosres.2016.07.018, 2016.

726 Fu, P., Kawamura, K., Kobayashi, M., and Simoneit, B. R.: Seasonal variations of sugars in atmospheric particulate
727 matter from Gosan, Jeju Island: Significant contributions of airborne pollen and Asian dust in spring, *Atmos.*
728 *environ.*, 55, 234–239, doi:10.1029/2003JD003697, 2012.

729 Fuzzi, S., Andreae, M. O., Huebert, B. J., Kulmala, M., Bond, T. C., Boy, M., Doherty, S. J., Guenther, A.,
730 Kanakidou, M., and Kawamura, K.: Critical assessment of the current state of scientific knowledge, terminology,
731 and research needs concerning the role of organic aerosols in the atmosphere, climate, and global change, *Atmos.*
732 *Chem. Phys.*, 22, doi:10.5194/acp-6-2017-2006, 2006.

733 Fuzzi, S., Baltensperger, U., Carslaw, K., Decesari, S., Denier van der Gon, H., Facchini, M. C., Fowler, D., Koren,
734 I., Langford, B., Lohmann, U., Nemitz, E., Pandis, S., Riipinen, I., Rudich, Y., Schaap, M., Slowik, J. G.,
735 Spracklen, D. V., Vignati, E., Wild, M., Williams, M., and Gilardoni, S.: Particulate matter, air quality and climate:
736 lessons learned and future needs, *Atmos. Chem. Phys.*, 15(14), 8217–8299, doi:10.5194/acp-15-8217-2015, 2015.

737 Gaston, C. J., Pratt, K. A., Qin, X., and Prather, K. A.: Real-time detection and mixing state of methanesulfonate
738 in single particles at an inland urban location during a phytoplankton bloom, *Environ. Sci. Technol.*, 44(5), 1566–
739 1572, doi:10.1021/es902069d, 2010.

740 Golly, B., Waked, A., Weber, S., Samaké, A., Jacob, V., Conil, S., Rangognio, J., Chrétien, E., Vagnot, M.-P.,
741 Robic, P.-Y., Besombes, J.-L., and Jaffrezo, J.-L.: Organic markers and OC source apportionment for seasonal
742 variations of PM_{2.5} at 5 rural sites in France, *Atmos. Environ.*, 198, 142–157, doi:10.1016/j.atmosenv.2018.10.027,
743 2018.

744 Gosselin, M. I., Rathnayake, C. M., Crawford, I., Pöhlker, C., Fröhlich-Nowoisky, J., Schmer, B., Després, V. R.,
745 Engling, G., Gallagher, M., Stone, E., Pöschl, U., and Huffman, J. A.: Fluorescent bioaerosol particle, molecular
746 tracer, and fungal spore concentrations during dry and rainy periods in a semi-arid forest, *Atmos. Chem. Phys.*,
747 16(23), 15165–15184, doi:10.5194/acp-16-15165-2016, 2016.

748 Heald, C. L., Coe, H., Jimenez, J. L., Weber, R. J., Bahreini, R., Middlebrook, A. M., Russell, L. M., Jolleys, M.,
749 Fu, T.-M., Allan, J. D., Bower, K. N., Capes, G., Crosier, J., Morgan, W. T., Robinson, N. H., Williams, P. I.,
750 Cubison, M. J., DeCarlo, P. F., and Dunlea, E. J.: Exploring the vertical profile of atmospheric organic aerosol:
751 comparing 17 aircraft field campaigns with a global model, *Atmos. Chem. Phys.*, 11(24), 12673–12696,
752 doi:10.5194/acp-11-12673-2011, 2011.

753 Hill, T. C. J., DeMott, P. J., Conen, F., and Möhler, O.: Impacts of bioaerosols on atmospheric ice nucleation
754 Processes, in *Microbiology of Aerosols*, pp. 195–219, John Wiley & Sons, Ltd.,
755 https://doi.org/10.1002/9781119132318, 2017.

756 Hiranuma, N., Adachi, K., Bell, D. M., Belosi, F., Beydoun, H., Bhaduri, B., Bingemer, H., Budke, C., Clemen,
757 H.-C., Conen, F., Cory, K. M., Curtius, J., DeMott, P. J., Eppers, O., Grawe, S., Hartmann, S., Hoffmann, N.,
758 Höhler, K., Jantsch, E., Kiselev, A., Koop, T., Kulkarni, G., Mayer, A., Murakami, M., Murray, B. J., Nicosia, A.,
759 Petters, M. D., Piazza, M., Polen, M., Reicher, N., Rudich, Y., Saito, A., Santachiara, G., Schiebel, T., Schill, G.
760 P., Schneider, J., Segev, L., Stopelli, E., Sullivan, R. C., Suski, K., Szakáll, M., Tajiri, T., Taylor, H., Tobo, Y.,
761 Ullrich, R., Weber, D., Wex, H., Whale, T. F., Whiteside, C. L., Yamashita, K., Zelenyuk, A., and Möhler, O.: A
762 comprehensive characterization of ice nucleation by three different types of cellulose particles immersed in water,
763 *Atmos. Chem. Phys.*, 19(7), 4823–4849, doi:10.5194/acp-19-4823-2019, 2019.

764 Hryniewicz, K., Baum, C., and Leinweber, P.: Density, metabolic activity, and identity of cultivable rhizosphere
765 bacteria on *Salix viminalis* in disturbed arable and landfill soils, *J. Plant Nutr. Soil Sci.*, 173(5), 747–756,
766 doi:10.1002/jpln.200900286, 2010.

767 Hsieh, T. C., Ma, K. H. and Chao, A.: iNEXT: an R package for rarefaction and extrapolation of species diversity
768 (Hill numbers), *Methods Ecol. Evol.*, 7(12), 1451–1456, doi:10.1111/2041-210X.12613, 2016.

769 Huerta-Cepas, J., Serra, F. and Bork, P.: ETE 3: Reconstruction, analysis, and visualization of Phylogenomic Data,
770 *Mol. Biol. Evol.*, 33(6), 1635–1638, doi:10.1093/molbev/msw046, 2016.

771 Huffman, J. A. and Santarpia, J.: Online techniques for quantification and characterization of biological aerosols,
772 in *Microbiology of Aerosols*, pp. 83–114, John Wiley & Sons, Ltd., https://doi.org/10.1002/9781119132318, 2017.

773 Huffman, J. A., Perring, A. E., Savage, N. J., Clot, B., Crouzy, B., Tummon, F., Shoshanim, O., Damit, B.,
774 Schneider, J., Sivaprakasam, V., Zawadowicz, M. A., Crawford, I., Gallagher, M., Topping, D., Doughty, D. C.,
775 Hill, S. C., and Pan, Y.: Real-time sensing of bioaerosols: review and current perspectives, *Aerosol Science and*
776 *Technology*, 1–31, doi:10.1080/02786826.2019.1664724, 2019.

777 Itävaara, M., Salavirta, H., Marjamaa, K., and Ruskeeniemi, T.: Geomicrobiology and metagenomics of Terrestrial
778 Deep Subsurface Microbiomes, in *Advances in Applied Microbiology*, vol. 94, pp. 1–77, Elsevier.,
779 doi:10.1016/bs.aambs.2015.12.001, 2016.

780 James, T. Y., Kauff, F., Schoch, C. L., Matheny, P. B., Hofstetter, V., Cox, C. J., Celio, G., Gueidan, C., Fraker,
781 E., Miadlikowska, J., Lumbsch, H. T., Rauhut, A., Reeb, V., Arnold, A. E., Amtoft, A., Stajich, J. E., Hosaka, K.,
782 Sung, G.-H., Johnson, D., O'Rourke, B., Crockett, M., Binder, M., Curtis, J. M., Slot, J. C., Wang, Z., Wilson, A.
783 W., Schüßler, A., Longcore, J. E., O'Donnell, K., Mozley-Standridge, S., Porter, D., Letcher, P. M., Powell, M.
784 J., Taylor, J. W., White, M. M., Griffith, G. W., Davies, D. R., Humber, R. A., Morton, J. B., Sugiyama, J.,
785 Rossman, A. Y., Rogers, J. D., Pfister, D. H., Hewitt, D., Hansen, K., Hambleton, S., Shoemaker, R. A.,
786 Kohlmeyer, J., Volkmann-Kohlmeyer, B., Spotts, R. A., Serdani, M., Crous, P. W., Hughes, K. W., Matsuura, K.,
787 Langer, E., Langer, G., Untereiner, W. A., Lücking, R., Büdel, B., Geiser, D. M., Aptroot, A., Diederich, P.,
788 Schmitt, I., Schultz, M., Yahr, R., Hibbett, D. S., Lutzoni, F., McLaughlin, D. J., Spatafora, J. W., and Vilgalys,
789 R.: Reconstructing the early evolution of Fungi using a six-gene phylogeny, *Nature*, 443(7113), 818–822,
790 doi:10.1038/nature05110, 2006.

791 Jia, Y., Bhat, S., and Fraser, M. P.: Characterization of saccharides and other organic compounds in fine particles
792 and the use of saccharides to track primary biologically derived carbon sources, *Atmos. Environ.*, 44(5), 724–732,
793 doi:10.1016/j.atmosenv.2009.10.034, 2010a.

794 Jia, Y., Clements, A. L. and Fraser, M. P.: Saccharide composition in atmospheric particulate matter in the
795 southwest US and estimates of source contributions, *J. Aerosol Sci.*, 41(1), 62–73,
796 doi:10.1016/j.jaerosci.2009.08.005, 2010b.

797 Jiang, W., Liang, P., Wang, B., Fang, J., Lang, J., Tian, G., Jiang, J., and Zhu, T. F.: Optimized DNA extraction
798 and metagenomic sequencing of airborne microbial communities, *Nat. Protoc.*, 10(5), 768–779,
799 doi:10.1038/nprot.2015.046, 2015.

800 Jocteur Monrozier, L., Guez, P., Chalamet, A., Bardin, R., Martins, J., and Gaudet, J. P.: Distribution of
801 microorganisms and fate of xenobiotic molecules in unsaturated soil environments, *Sci. Total Environ.*, 136(1–2),
802 121–133, doi:10.1016/0048-9697(93)90302-M, 1993.

803 Kang, M., Ren, L., Ren, H., Zhao, Y., Kawamura, K., Zhang, H., Wei, L., Sun, Y., Wang, Z., and Fu, P.: Primary
804 biogenic and anthropogenic sources of organic aerosols in Beijing, China: insights from saccharides and n-alkanes,
805 *Environ. Pollut.*, 243, 1579–1587, doi:10.1016/j.envpol.2018.09.118, 2018.

806 Kelly, F. J. and Fussell, J. C.: Air pollution and public health: emerging hazards and improved understanding of
807 risk, *Environ. Geochem. Health*, 37(4), 631–649, doi:10.1007/s10653-015-9720-1, 2015.

808 Kuffner, M., De Maria, S., Puschenreiter, M., Fallmann, K., Wieshammer, G., Gorfer, M., Strauss, J., Rivelli, A.
809 R., and Sessitsch, A.: Culturable bacteria from Zn- and Cd-accumulating *Salix caprea* with differential effects on
810 plant growth and heavy metal availability, *J. Appl. Microbiol.*, 108(4), 1471–1484, doi:10.1111/j.1365-
811 2672.2010.04670.x, 2010.

812 Lecours, P. B., Duchaine, C., Thibaudon, M., and Marsolais, D.: Health impacts of bioaerosol exposure, in
813 *Microbiology of Aerosols*, pp. 249–268, John Wiley & Sons, Ltd., <https://doi.org/10.1002/9781119132318>, 2017.

814 Liu, H., Hu, Z., Zhou, M., Hu, J., Yao, X., Zhang, H., Li, Z., Lou, L., Xi, C., Qian, H., Li, C., Xu, X., Zheng, P.,
815 and Hu, B.: The distribution variance of airborne microorganisms in urban and rural environments, *Environ.*
816 *Pollut.*, 247, 898–906, doi:10.1016/j.envpol.2019.01.090, 2019.

817 Luhung, I., Wu, Y., Ng, C. K., Miller, D., Cao, B., and Chang, V. W.-C.: Protocol improvements for low
818 concentration DNA-based bioaerosol sampling and analysis, *PLOS ONE*, 10(11), e0141158,
819 doi:10.1371/journal.pone.0141158, 2015.

820 Lymperopoulou, D. S., Adams, R. I., and Lindow, S. E.: Contribution of vegetation to the microbial composition
821 of nearby outdoor air, *Appl. Environ. Microbiol.*, 82(13), 3822–3833, doi:10.1128/AEM.00610-16, 2016.

822 Maron, P.-A., Lejon, D. P. H., Carvalho, E., Bizet, K., Lemanceau, P., Ranjard, L., and Mougel, C.: Assessing
823 genetic structure and diversity of airborne bacterial communities by DNA fingerprinting and 16S rDNA clone
824 library, *Atmos. Environ.*, 39(20), 3687–3695, doi:10.1016/j.atmosenv.2005.03.002, 2005.

825 McMurdie, P. J. and Holmes, S.: phyloseq: An R package for reproducible interactive analysis and graphics of
826 microbiome sensus Data, *PLoS ONE*, 8(4), e61217, doi:10.1371/journal.pone.0061217, 2013.

827 Medeiros, P. M., Conte, M. H., Weber, J. C., and Simoneit, B. R. T.: Sugars as source indicators of biogenic
828 organic carbon in aerosols collected above the howland experimental forest, Maine, *Atmos. Environ.*, 40(9), 1694–
829 1705, doi: doi.org/10.1016/j.atmosenv.2005.11.001, 2006.

830 Mercier, C., Boyer, F., Kopylova, E., Taberlet, P., Bonin, A., and Coissac, E.: SUMATRA and SUMACLUSt:
831 fast and exact comparison and clustering of sequences. Programs and Abstracts of the SeqBio, Workshop, pp. 27–
832 29., 2013.

833 Mhuireach, G., Johnson, B. R., Altrichter, A. E., Ladau, J., Meadow, J. F., Pollard, K. S., and Green, J. L.: Urban
834 greenness influences airborne bacterial community composition, *Sci. Total Environ.*, 571, 680–687,
835 doi:10.1016/j.scitotenv.2016.07.037, 2016.

836 Moore, D., Robson, G. D., and Trinci, A. P. J.: 21st century guidebook to fungi, Cambridge University Press,
837 Cambridge., <https://doi.org/10.1017/CBO9780511977022>, 2011.

838 Ng, T. W., Ip, M., Chao, C. Y. H., Tang, J. W., Lai, K. P., Fu, S. C., Leung, W. T., and Lai, K. M.: Differential
839 gene expression in *Escherichia coli* during aerosolization from liquid suspension, *Appl. Microbiol. Biotechnol.*,
840 102(14), 6257–6267, doi:10.1007/s00253-018-9083-5, 2018.

841 Ofek, M., Hadar, Y. and Minz, D.: Ecology of root colonizing massilia (oxalobacteraceae), *PLoS ONE*, 7(7),
842 e40117, doi:10.1371/journal.pone.0040117, 2012.

843 Oksanen, J., Blanchet, F. G., Friendly, M., Kindt, R., Legendre, P., McGlenn, D., R. Minchin, P. R., O’Hara, R.
844 B., Simpson, G. L., Solymos, Peter, Stevens, M. H. H., Szoecs, E., and Wagner, H.: Vegan: community ecology
845 package, <https://cran.r-project.org>, <https://github.com/vegandevs/vegan>, 2019.

846 Oliveira, M., Ribeiro, H., Delgado, J. L., and Abreu, I.: The effects of meteorological factors on airborne fungal
847 spore concentration in two areas differing in urbanisation level, *Int. J. Biometeorol.*, 53(1), 61–73,
848 doi:10.1007/s00484-008-0191-2, 2009.

849 Prather, K. A., Bertram, T. H., Grassian, V. H., Deane, G. B., Stokes, M. D., DeMott, P. J., Aluwihare, L. I.,
850 Palenik, B. P., Azam, F., Seinfeld, J. H., Moffet, R. C., Molina, M. J., Cappa, C. D., Geiger, F. M., Roberts, G. C.,
851 Russell, L. M., Ault, A. P., Baltrusaitis, J., Collins, D. B., Corrigan, C. E., Cuadra-Rodriguez, L. A., Ebben, C. J.,
852 Forestieri, S. D., Guasco, T. L., Hersey, S. P., Kim, M. J., Lambert, W. F., Modini, R. L., Mui, W., Pedler, B. E.,
853 Ruppel, M. J., Ryder, O. S., Schoepp, N. G., Sullivan, R. C., and Zhao, D.: Bringing the ocean into the laboratory
854 to probe the chemical complexity of sea spray aerosol, *Proc Natl Acad Sci U S A*, 110(19), 7550–7555,
855 doi:10.1073/pnas.1300262110, 2013.

856 Pietrogrande, M. C., Bacco, D., Visentin, M., Ferrari, S., and Casali, P.: Polar organic marker compounds in
857 atmospheric aerosol in the Po valley during the Supersito campaigns — part 2: seasonal variations of sugars,
858 *Atmos. Environ.*, 97, 215–225, doi:10.1016/j.atmosenv.2014.07.056, 2014.

859 Pope, C. A. and Dockery, D. W.: Health effects of fine particulate air pollution: lines that connect, *J. Air Waste*
860 *Manag. Assoc.*, 56(6), 709–742, 2006.

861 Rastogi, G., Coaker, G. L., and Leveau, J. H. J.: New insights into the structure and function of phyllosphere
862 microbiota through high-throughput molecular approaches, *FEMS Microbiol. Lett.*, 348(1), 1–10,
863 doi:10.1111/1574-6968.12225, 2013.

864 Rathnayake, C. M., Metwali, N., Baker, Z., Jayarathne, T., Kostle, P. A., Thorne, P. S., O’Shaughnessy, P. T., and
865 Stone, E. A.: Urban enhancement of PM₁₀ bioaerosol tracers relative to background locations in the midwestern
866 United States, *J. Geophys. Res. Atmos.*, 121(9), 5071–5089, doi:10.1002/2015JD024538, 2016.

867 Samaké, A.; Uzu, G.; Martins, J.M.F.; Calas, A.; Vince, E.; Parat, S.; and Jaffrezo, J.L. The unexpected role of
868 bioaerosols in the Oxidative Potential of PM. *Sci. Rep.*, 7, 10978, doi:10.1038/s41598-017-11178-0, 2017.

869 Samaké, A., Jaffrezo, J.-L., Favez, O., Weber, S., Jacob, V., Canete, T., Albinet, A., Charron, A., Riffault, V.,
870 Perdrix, E., Waked, A., Golly, B., Salameh, D., Chevrier, F., Oliveira, D. M., Besombes, J.-L., Martins, J. M. F.,
871 Bonnaire, N., Conil, S., Guillaud, G., Mesbah, B., Rocq, B., Robic, P.-Y., Hulin, A., Le Meur, S., Descheemaeker,
872 M., Chretien, E., Marchand, N., and Uzu, G.: Arabitol, mannitol, and glucose as tracers of primary biogenic organic
873 aerosol: the influence of environmental factors on ambient air concentrations and spatial distribution over France,
874 *Atmos. Chem. Phys.*, 19(16), 11013–11030, doi:10.5194/acp-19-11013-2019, 2019a.

875 Samaké, A., Jaffrezo, J.-L., Favez, O., Weber, S., Jacob, V., Albinet, A., Riffault, V., Perdrix, E., Waked, A.,
876 Golly, B., Salameh, D., Chevrier, F., Oliveira, D. M., Bonnaire, N., Besombes, J.-L., Martins, J. M. F., Conil, S.,
877 Guillaud, G., Mesbah, B., Rocq, B., Robic, P.-Y., Hulin, A., Le Meur, S., Descheemaeker, M., Chretien, E.,
878 Marchand, N., and Uzu, G.: Polyols and glucose particulate species as tracers of primary biogenic organic aerosols
879 at 28 French sites, *Atmos. Chem. Phys.*, 19(5), 3357–3374, doi:10.5194/acp-19-3357-2019, 2019b.

880 Schnell, I. B., Bohmann, K., and Gilbert, M. T. P.: Tag jumps illuminated - reducing sequence-to-sample
881 misidentifications in metabarcoding studies, *Mol. Ecol. Resour.*, 15(6), 1289–1303, doi:10.1111/1755-
882 0998.12402, 2015.

883 Taberlet, P., Bonin, A., Zinger, L., and Coissac, E.: *Environmental DNA: for biodiversity research and monitoring*,
884 Oxford University Press, Oxford, New York., DOI:10.1093/oso/9780198767220.001.0001, 2018.

885 Verma, S. K., Kawamura, K., Chen, J., and Fu, P.: Thirteen years of observations on primary sugars and sugar
886 alcohols over remote Chichijima Island in the western north pacific, *Atmos. Chem. Phys.*, 18(1), 81–101,
887 doi:https://doi.org/10.5194/acp-18-81-2018, 2018.

888 Waked, A., Favez, O., Alleman, L. Y., Piot, C., Petit, J.-E., Delaunay, T., Verlinden, E., Golly, B., Besombes, J.-
889 L., Jaffrezo, J.-L., and Leoz-Garziandia, E.: Source apportionment of PM₁₀ in a north-western Europe regional
890 urban background site (Lens, France) using positive matrix factorization and including primary biogenic
891 emissions, *Atmos. Chem. Phys.*, 14(7), 3325–3346, doi:10.5194/acp-14-3325-2014, 2014.

892 Weber, S., Uzu, G., Calas, A., Chevrier, F., Besombes, J.-L., Charron, A., Salameh, D., Ježek, I., Močnik, G. and
893 Jaffrezo, J.-L.: An apportionment method for the oxidative potential of atmospheric particulate matter sources:
894 application to a one-year study in Chamonix, France, *Atmos. Chem. Phys.*, 18(13), 9617–9629, doi:10.5194/acp-
895 18-9617-2018, 2018.

896 Wei, M., Xu, C., Xu, X., Zhu, C., Li, J., and Lv, G.: Characteristics of atmospheric bacterial and fungal
897 communities in PM_{2.5} following biomass burning disturbance in a rural area of North China Plain, *Sci. Total*
898 *Environ.*, 651, 2727–2739, doi:10.1016/j.scitotenv.2018.09.399, 2019a.

899 Wei, M., Xu, C., Xu, X., Zhu, C., Li, J., and Lv, G.: Size distribution of bioaerosols from biomass burning
900 emissions: characteristics of bacterial and fungal communities in submicron (PM_{1.0}) and fine (PM_{2.5}) particles,
901 *Ecotoxicol. Environ. Saf.*, 171, 37–46, doi:10.1016/j.ecoenv.2018.12.026, 2019b.

902 Weinert, N., Meincke, R., Gottwald, C., Radl, V., Dong, X., Schloter, M., Berg, G., and Smalla, K.: Effects of
903 genetically modified potatoes with increased zeaxanthin content on the abundance and diversity of rhizobacteria
904 with in vitro antagonistic activity do not exceed natural variability among cultivars, *Plant Soil*, 326(1–2), 437–
905 452, doi:10.1007/s11104-009-0024-z, 2010.

906 Welsh, D. T.: Ecological significance of compatible solute accumulation by micro-organisms: from single cells to
907 global climate, *FEMS Microbiol. Rev.*, 24(3), 263–290, doi:10.1111/j.1574-6976.2000.tb00542.x, 2000.

908 Womack, A. M., Artaxo, P. E., Ishida, F. Y., Mueller, R. C., Saleska, S. R., Wiedemann, K. T., Bohannon, B. J.
909 M., and Green, J. L.: Characterization of active and total fungal communities in the atmosphere over the amazon
910 rainforest, *Biogeosciences*, 12(21), 6337–6349, doi:10.5194/bg-12-6337-2015, 2015.

911 Xu, C., Wei, M., Chen, J., Zhu, C., Li, J., Lv, G., Xu, X., Zheng, L., Sui, G., Li, W., Chen, B., Wang, W., Zhang,
912 Q., Ding, A. and Mellouki, A.: Fungi diversity in PM_{2.5} and PM₁ at the summit of Mt. Tai: abundance, size
913 distribution, and seasonal variation, *Atmos. Chem. Phys.*, 17(18), 11247–11260, doi:10.5194/acp-17-11247-2017,
914 2017.

915 Xue, C., Liu, T., Chen, L., Li, W., Liu, I., Kronstad, J. W., Seyfang, A. and Heitman, J.: Role of an expanded
916 inositol transporter repertoire in *Cryptococcus neoformans* sexual reproduction and virulence, 1(1),
917 doi:10.1128/mBio.00084-10, 2010.

918 Yadav, A. N., Verma, P., Sachan, S. G., Kaushik, R., and Saxena, A. K.: Psychrotrophic microbiomes: molecular
919 diversity and beneficial role in plant growth promotion and soil health, in *Microorganisms for Green Revolution*,
920 vol. 7, pp. 197–240, Springer Singapore, Singapore., doi: 10.1007/978-981-10-7146-1-11, 2018.

921 Yang, Y., Chan, C., Tao, J., Lin, M., Engling, G., Zhang, Z., Zhang, T., and Su, L.: Observation of elevated fungal
922 tracers due to biomass burning in the Sichuan Basin at Chengdu City, China, *Sci. Total Environ.*, 431, 68–77,
923 2012.

924 Yan, C., Sullivan, A. P., Cheng, Y., Zheng, M., Zhang, Y., Zhu, T., and Collett, J. L.: Characterization of
925 saccharides and associated usage in determining biogenic and biomass burning aerosols in atmospheric fine
926 particulate matter in the North China Plain, *Sci. Total Environ.*, 650, 2939–2950,
927 doi:10.1016/j.scitotenv.2018.09.325, 2019.

928 Yu, X., Wang, Z., Zhang, M., Kuhn, U., Xie, Z., Cheng, Y., Pöschl, U., and Su, H.: Ambient measurement of
929 fluorescent aerosol particles with a WBS in the Yangtze River Delta of China: potential impacts of combustion-
930 related aerosol particles, *Atmos. Chem. Phys.*, 16(17), 11337–11348, doi:10.5194/acp-16-11337-2016, 2016.

931 Zhu, C., Kawamura, K., and Kunwar, B.: Organic tracers of primary biological aerosol particles at subtropical
932 Okinawa Island in the western North Pacific Rim: organic biomarkers in the north Pacific, *Journal of Geophysical
933 Research: Atmospheres*, 120(11), 5504–5523, 2015.

934